the Institute of Laboratory Animals of the Graduate School of Medicine, Kyoto University. All of the experimental procedures were performed in accordance with the National Institutes of Health (NIH) Guide for the Care and Use of Laboratory Animals. We intended to minimize the numbers of animals and their suffering.

### EP4 mRNA expression in mouse cochleae

Under general anesthesia with midazolam (10 mg/kg; Astellas, Tokyo, Japan) and xylazine (10 mg/kg; Bayer, Tokyo, Japan), mice were sacrificed and their cochleae were immediately collected. Each mouse cochlea was homogenized, and total RNA was extracted using an RNeasy mini kit (Qiagen Ltd., Valencia, CA, USA). Complementary DNA was synthesized from DNase I-treated total RNA using the Superscript first-strand synthesis kit (Invitrogen, Carlsbad, CA, USA). Polymerase chain reaction (PCR) was performed using a GeneAmp PCR system 9700 (Perkin Elmer Applied Biosystems, Foster City, CA, USA). The primers used in the PCR for EP4 and for β-actin as an invariant control were as follows: EP4 (424 base pairs [bp]), 5′-TTCCGCTCGTGGTGCGAGTGTTC-3′ (sense) and 5′-GAGGTGGTGTCTGCTTGGGTACG-3′ (antisense); and β-actin (321 bp), 5′-ACCAACTGGGACGACATGGAGAAGATCTGG-3′ (sense) and 5′-CCGGCCAGCCAGGTCCAGACGCAGGATGGC-3′ (antisense). The PCR conditions for EP4 were as follows: denaturation at 94 °C for 48 s, annealing at 64 °C for 42 s, and extension at 72 °C for 25 s. The PCR conditions for β-actin were as follows: denaturation at 94 °C for 48 s, annealing at 62 °C for 42 s, and extension at 72 °C for 72 s. The numbers of PCR cycles were 35 and 30 for EP4 and β-actin, respectively. All reactions were confirmed to be in the logarithmic phase by monitoring the PCR products obtained at the indicated number of cycles (±2). The PCR products were electrophoresed on a 1.5% agarose gel and stained with ethidium bromide. The RT-PCR experiments were independently repeated three times using the same total RNA material. Extracts of mouse lungs were used as positive controls, and negative controls were obtained by omitting reverse transcriptase from the reactions.

### Immunohistochemistry for EP4 in the cochlea

Immunohistochemistry was performed to examine the localization of EP4 in the auditory epithelia. Cochlear specimens from the mice were fixed with 4% paraformaldehyde (PFA) in 0.01 M phosphate-buffered saline (PBS; pH 7.4) at 4 °C for 12 h. After decalcification with 0.1 M EDTA for 7 days at 4 °C, 10-μm-thick cryostat sections were prepared. Anti-EP4 receptor polyclonal antibody (dilution, 1:200; Cayman Chemical, Ann Arbor, MI, USA) was used as the primary antibody for 12 h at 4 °C, and Alexa 568–conjugated goat anti-rabbit immunoglobulin G (dilution, 1:500; Molecular Probes, Eugene, OR, USA) was used as the secondary antibody for 1 h at room temperature. After immunostaining for EP4, the nuclei were counterstained with 4,6-diamidino,2-phenylindole dihydrochloride (DAPI; 1 μg/ml in PBS; Molecular Probes). Heart specimens obtained from the mice were used as positive controls for EP4. Nonspecific labeling was tested by blocking protein–antibody complex formation using EP4 receptor blocking peptide (Cayman Chemical). The specimens were viewed with a Leica TCS-SPE confocal microscope (Leica Microsystems, Wetzlar, Germany).

### Drug application and noise exposure

The EP4 agonist used was ONO-AE1-329 (Ono Pharmaceutical, Co., Ltd., Osaka, Japan). After the ABR measurements, the otic bulla of the left temporal bone of each guinea pig was exposed using a retroauricular approach under general anesthesia with midazolam (10 mg/kg i.m.) and xylazine (10 mg/kg i.m.). A small hole was made in the left bulla to expose the round window niche. A gelatin sponge in dry conditions was cut into pieces 1.5–2 $mm^3$ in size under microscopy. A piece of gelatin that had been immersed in the EP4 agonist, which had been dissolved in dimethyl sulfoxide (DMSO) and diluted with physiological saline to give a final concentration of 1 mg/ml containing 1% DMSO, was then placed on the round window membrane (RWM) of the animals in the EP4 agonist group ($n$=8). For the animals in the control group, a piece of gelatin that had been immersed in physiological saline containing 1% DMSO was used ($n$=9). The animals were exposed to one octave band noise centered on 4 kHz at a sound pressure level (SPL) of 120 dB for 5 h in a ventilated sound-exposure chamber immediately after drug application under general anesthesia with midazolam and xylazine. Each animal was immobilized, and a speaker was centered over the animal's head at a distance of 15 cm. The sound chamber was fitted with speakers driven by a noise generator and a power amplifier. Using a 1/2-inch condenser microphone (Sony, Tokyo, Japan) and fast Fourier transform analyzer (Sony), sound levels were monitored and calibrated at multiple locations within the sound chamber to ensure uniformity of the stimulus. The stimulus intensity varied by a maximum of 3 dB SPL across measured sites within the exposure chamber. We also examined post-treatment effects. The animals were locally administered an EP4 agonist ($n$=5) or physiological saline containing 1% DMSO ($n$=5) 30 min after noise exposure. ABR thresholds following local application of saline containing 1% DMSO were measured in normal guinea pigs ($n$=4) as a control experiments.

### ABR measurements

The ABR thresholds were measured at frequencies of 4, 8, and 16 kHz before noise exposure, and on days 3, 7, 14 and 21 after drug application. The animals were anesthetized with midazolam and xylazine, and kept warm with a heating pad. The generation of acoustic stimuli and the subsequent recording of evoked potentials were performed using a Powerlab/4sp (ADInstruments, Colorad Springs, CO, USA). The acoustic stimuli, which consisted of tone-burst stimuli (0.1 ms cos2 rise/fall and 1-ms plateau), were delivered monaurally through a speaker (ES1spc; Bioresearch Center, Nagoya, Japan) connected to a funnel fitted into the external auditory meatus. To record bioelectrical potentials, subdermal stainless-steel needle electrodes were inserted at the vertex (ground), ventrolateral to the measured ear (active), and contralateral to the measured ear (reference). The stimuli were calibrated against a 3-inch free-field microphone (ACO-7016; ACO Pacific, Belmont, CA, USA) connected to an oscilloscope (DS-8812 DS-538; Iwatsu Electric, Tokyo, Japan) or a sound level meter (LA-5111; Ono Sokki, Yokohama, Japan). The thresholds were determined from a set of responses at varying intensities with 5-dB SPL intervals, and the electrical signals were averaged over 1024 repetitions. The thresholds at each frequency were verified at least twice.

### Histological analyses

On day 21 after drug application, the temporal bones were collected and immersed in 4% PFA in 0.01 M PBS at 4 °C for 12 h. After decalcification with 0.1 M EDTA for 14 days at 4 °C, the cochleae were subjected to histological analysis as whole mounts. Three regions of the cochlear sensory epithelia, at a distance of 30%–50% (corresponding to 1–3 kHz regions, second turn), 50%–70% (corresponding to 3–8 kHz regions, mid-basal portion), and 70%–90% (corresponding to 8–30 kHz regions, basal portion) from the apex (Viberg and Canlon, 2004), were used for quantitative assessments of HC loss. Cochlear specimens were permeabilized in 0.2% Triton X in PBS for 30 min at room temperature. Immunohistochemistry for myosin VIIa and F-actin labeling by phalloidin were used to label the inner hair cells (IHCs) and the outer hair cells (OHCs). Anti-myosin VIIa rabbit polyclonal antibody (dilution, 1:500; Proteus BioSciences, Ramona, CA, USA)

was used as the primary antibody for 12 h at 4 °C, and Alexa 568–conjugated goat anti-rabbit immunoglobulin G (dilution, 1:500) was used as the secondary antibody for 1 h at room temperature. After immunostaining for myosin VIIa, the specimens were stained with fluorescein–phalloidin (1:400; Molecular Probes) for 15 min at room temperature. Specimens were viewed under confocal microscopy (TCS SP2; Leica Microsystems, Wetzlar, Germany). Nonspecific labeling was tested by omitting the primary antibody from the staining procedures. The numbers of IHCs and OHCs in 0.2-mm-long regions of each region of the cochleae were counted by the three authors (R.H., T.N., and T.S.). The average of these values was used for each animal. The samples obtained from eight animals pre-treated with an EP4 agonist, nine animals pre-treated with saline containing DMSO, five animals post-treated with an EP4 agonist and five animals post-treated with saline containing DMSO were provided for statistical analyses.

### Statistical analysis

The overall effects of EP4 agonist application on ABR threshold shifts were examined using two-way factorial analysis of variance. When the interactions were significant, multiple comparisons using the Fisher protected least significant difference test were performed for pairwise comparisons. Differences in the numbers of IHCs and OHCs in each region between the EP4 agonist-treated cochleae and the control cochleae were examined using the Student's *t*-test. *P*-values $<0.05$ were considered statistically significant. Values are expressed as the mean and the standard error of the mean (SEM).

## RESULTS

### EP4 expression in cochleae

RT-PCR analysis of the EP4 mRNA levels was performed to investigate EP4 expression. Amplification of β-actin, yielding a 321-bp amplicon, was used as an internal control (Fig. 1). Negative control reactions that lacked reverse transcriptase failed to yield amplicons of either β-actin or EP4 (lane 3 in Fig. 1). We used the mouse lung as a positive control for EP4, which exhibited EP4 mRNA expression (lane 1 in Fig. 1). The mouse cochleae also demonstrated EP4 mRNA expression (lane 2 in Fig. 1). Immunostaining revealed that EP4 expression occurred in the stria vascularis, spiral ligament, spiral ganglion neurons, supporting cells, and HCs (Fig. 2A–C), while negative controls using a specific blocking peptide showed no immunoreactivity (Fig. 2D–F). These findings confirmed that EP4 expression was present in the cochlear cells, including the HCs.

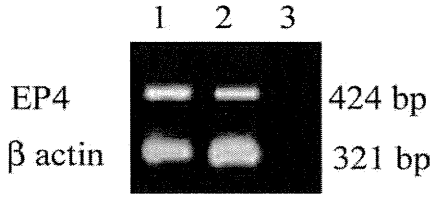


**Fig. 1.** RT-PCR for EP4 and β-actin expression in the inner ear. EP4 (424 bp band) was detected in mouse lung (lane 1) and cochleae (lane 2) specimens. β-Actin (321 bp band), as an invariant control, was detected in both types of specimen. No product was detected in specimens in the absence of the RT reaction (lane 3).

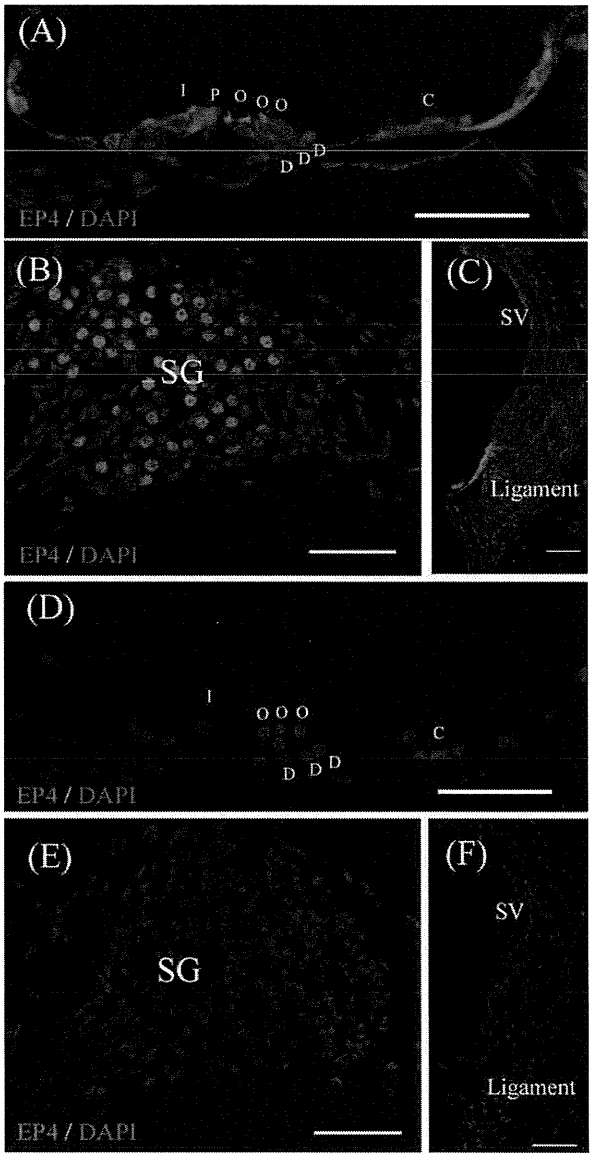


**Fig. 2.** Immunoreactivity for EP4 and counterstained nuclei. (A–C) EP4 expression was detected in the stria vascularis (SV), spiral ganglion cells (SG), sensory epithelium (I, IHC; O, OHC; D, Deiter's; C, Claudius' cell; P, pillar cell). In negative controls that were stained after blocking with specific peptide (D–F), no immunoreactivity for EP4 is found in the cochlea. Scale bar=200 μm.

### ABR threshold shifts

Local application of saline containing 1% DMSO in normal guinea pigs showed no significant elevation of ABR thresholds following drug application (data not shown). The time courses of alterations in the ABR threshold shifts in noise-exposed animals at 4, 8, and 16 kHz are shown in Fig. 3. For pre-treatment experiments, the data from eight animals treated with the EP4 agonist and that from nine animals treated with physiological saline containing DMSO were provided for statistical analyses. Local EP4 agonist treatment had significant effects on the ABR threshold shifts at each frequency. The overall effect of EP4 agonist application at 4, 8, and 16 kHz was significant ($P<0.0001$).

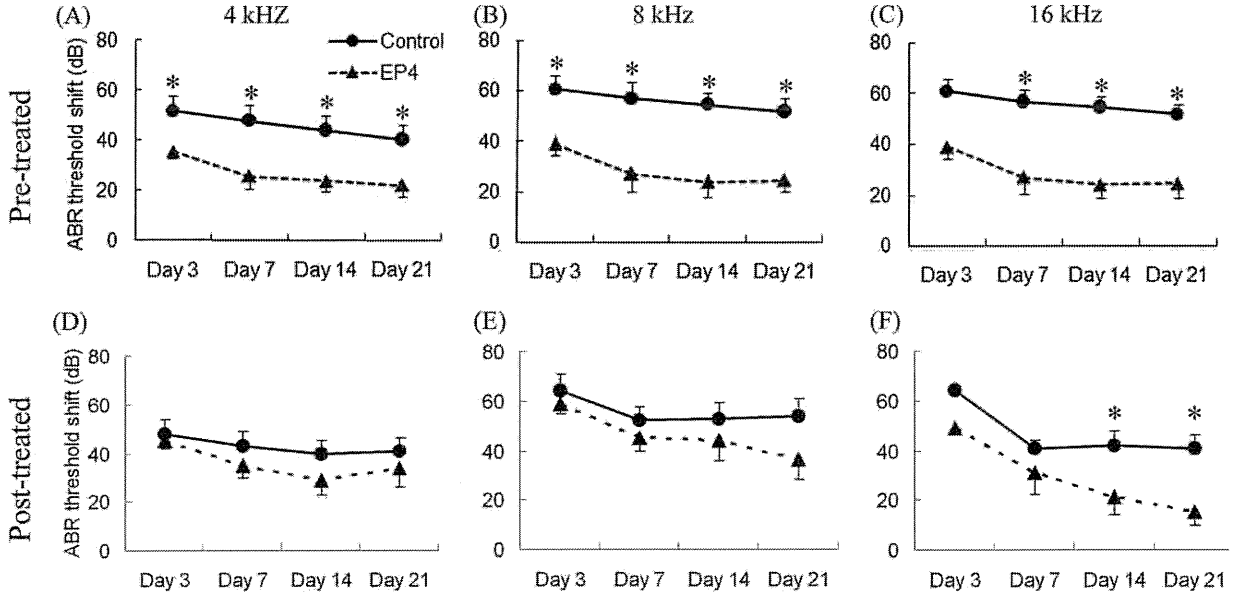


**Fig. 3.** Time courses of alterations in threshold shifts of ABRs in EP4 agonist-treated cochleae and control cochleae at frequencies of 4, 8, and 16 kHz in pre-treated animals (A–C) or in post-treated animals (D–F). In pre-treated animals, the overall effects at 4, 8, and 16 kHz of EP4 agonist application were significant ($P<0.0001$). The differences in ABR threshold shifts at 4 and 8 kHz between EP4 agonist-treated cochleae and control cochleae on days 3, 7, 14 and 21 were significant. The differences in ABR threshold shifts at 16 kHz on days 7, 14 and 21 were significant (* $P<0.05$). In post-treated animals, the overall effects at 8 and 16 kHz of EP4 agonist application were significant ($P=0.042$ for 8 kHz and $P<0.0001$ for 16 kHz). The differences in ABR threshold shifts at 16 kHz on days 14 and 21 were significant (* $P<0.05$). Bars represent the SEM.

The differences in the threshold shifts at 4 kHz between the EP4 agonist-treated cochleae and the control cochleae on days 3, 7, 14 and 21 were shown to be significant in multiple comparisons using the Fisher protected least significant difference test ($P=0.039$ for day 3, $P=0.005$ for day 7, $P=0.010$ for day 14, and $P=0.020$ for day 21). The differences in the threshold shifts at 8 kHz between the EP4 agonist-treated cochleae and the control cochleae were significant on days 3, 7, 14 and 21 ($P=0.008$ for day 3, $P<0.001$ for day 7, $P=0.010$ for day 14, and $P=0.001$ for day 21). The differences in the threshold shifts at 16 kHz between the EP4 agonist-treated cochleae and the control cochleae were significant on days 7, 14 and 21 ($P=0.017$ for day 7, $P=0.012$ for day 14, and $P=0.011$ for day 21), but not on day 3 ($P=0.117$). For post-treatment experiments, the data from five animals treated with the EP4 agonist and that from five animals treated with physiological saline containing DMSO were provided for statistical analyses. The overall effects of EP4 agonist application at 8 and 16 kHz were significant ($P=0.042$ for 8 kHz and $P<0.0001$ for 16 kHz), but not at 4 kHz. The differences in the threshold shifts at 16 kHz between the EP4 agonist-treated cochleae and the control cochleae on days 14 and 21 were shown to be significant in multiple comparisons ($P=0.008$ for day 14 and $P=0.003$ for day 21). No significant difference in ABR threshold shifts at 8 kHz was found in multiple comparisons. These findings indicate that local EP4 agonist treatment offered functional protection of the auditory system against noise-induced damage.

### HC protection

Immunostaining for myosin VIIa and phalloidin staining demonstrated severe degeneration of the OHCs in the second turn, mid-basal, and basal portions of the control cochleae (Fig. 4A, D, G); by contrast, the OHC degener-

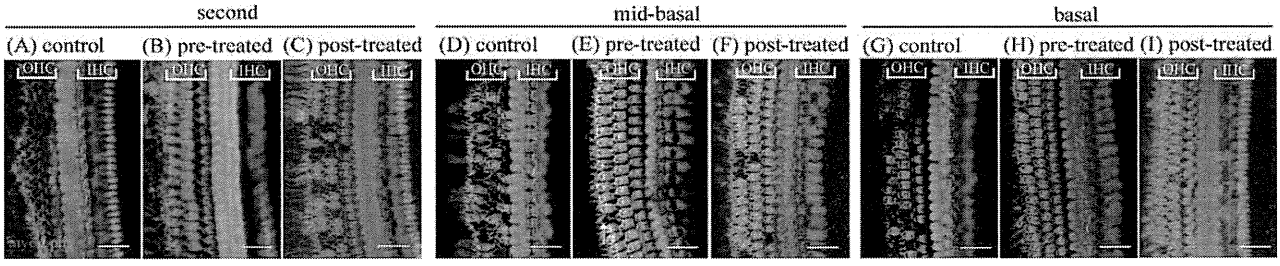


**Fig. 4.** Immunostaining for myosin VIIa (myo; red) and F-actin labeling with phalloidin (pha; green) of cochlear sensory epithelia in the second turn, mid-basal and basal portions. Severe loss of OHCs was observed in the control cochlea (A, D, G). Degeneration of OHCs was limited in the specimen pre-treated with an EP4 agonist (B, E, H). Moderate degeneration of OHCs was observed in the second turn and the mid-basal portion of the cochlea post-treated with an EP4 agonist (C, F, I). Scale bar=25 $\mu$m. For interpretation of the references to color in this figure legend, the reader is referred to the Web version of this article.

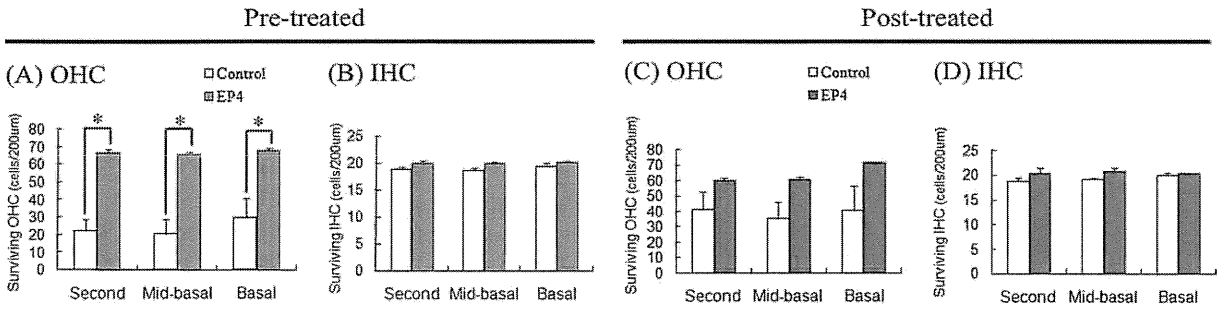


**Fig. 5.** Numbers of surviving OHCs and IHCs in the second turn, mid-basal and basal portions apical, middle, and basal portions of cochleae. Significant differences in the numbers of surviving OHCs were found between the EP4 agonist-treated cochleae and the control cochleae in all the portions in a pre-treated condition (A; * $P<0.01$). However, in a post-treated condition, significant differences in the numbers of OHCs were not found between the two groups (C). No significant differences in the numbers of IHCs were found between the two groups in either condition (B, D). Bars represent the SEM.

ation was limited in the cochleae pre-treated with an EP4 agonist (Fig. 4B, E, H). The IHCs were preserved in both experimental groups (Fig. 4A, B). Quantitative assessments revealed significant differences in the numbers of surviving OHCs in all cochlear portions between the cochleae pre-treated with an EP4 agonist and those pre-treated with saline containing DMSO (Fig. 5A). The differences in the numbers of surviving OHCs between the EP4 agonist-treated cochleae and the control cochleae were significant in the second turn ($P<0.001$), mid-basal ($P<0.001$), and basal portions ($P=0.006$). No significant differences were observed in the numbers of surviving IHCs between the EP4 agonist-treated cochleae and the control cochleae (Fig. 5B). In post-treatment experiments, the OHC degeneration in the cochleae post-treated with an EP4 agonist appeared to be moderate (Fig. 4C, F, I), however, quantitative assessments revealed no significant differences between the EP4 agonist-treated cochleae and the control cochleae (Fig. 5C). No significant differences in the numbers of surviving IHCs were also observed between the two groups in post-treatment experiments (Fig. 5D).

## DISCUSSION

$PGE_1$ has been applied to patients with idiopathic sudden SNHL; however, its clinical efficacy and its mechanism of action for this disease have not been determined. $PGE_1$ directly stimulates several signaling pathways via the PGI receptor (IP) and four subtypes of the PGE receptors (EP1-4), resulting in changes cAMP and phosphoinositide cellular levels (Kiriyama et al., 1997; Narumiya et al., 1999). The present results show the expression of EP4 in the cochlea, and the attenuation of noise-induced damage by local EP4 agonist administration, suggesting an involvement of EP4 in mechanisms for therapeutic effects of $PGE_1$ for SNHL. On the other hand, IP, EP2 and EP4 mediate an increase of intracellular cAMP levels, while the activation of the EP3 leads to a decrease of cAMP levels. Therefore, the stimulation of EP3 by $PGE_1$ may contradict effects of IP, EP2 or EP4 stimulation by $PGE_1$, indicating that selective antagonists for IP, EP2 or EP4 might be more effective for treatment of SNHL than $PGE_1$.

Recent studies have indicated the potential of EP4 agonists for neuro-protection. An *in vitro* study using primary culture of cortical neurons has revealed that EP4 agonists protect neurons against amyloid $\beta$-peptide toxicity via the cAMP–PKA pathway (Echeverria et al., 2005), which is also involved in mechanisms for promotion of the auditory neuron survival (Bok et al., 2003; Alam et al., 2007). An EP4 agonist, ONO-AE1-329, which was used in the present study, has been reported to attenuate brain injury due to glutamate excitotoxicity *in vivo* (Ahmad et al., 2005). Excitotoxicity mediated by glutamate receptors also plays an important role in mechanisms of cochlear damage induced by noise trauma and ischemic injury (Pujol et al., 1999; Ruel et al., 2007). These previous findings encouraged us to investigate protective effects of ONO-AE1-329 against noise trauma. As we expected, present findings demonstrate that local EP4 agonist treatment applied to the cochlea significantly reduced the elevation of the ABR thresholds and OHC loss, indicating the potential of an EP4 agonist, ONO-AE1-329, for cochlea protection similarly to the CNS.

There are several potential explanations for the mechanisms underlying otoprotection by EP4 agonists. One possible mechanism is a direct action of EP4 agonists on cochlear HCs. The stimulation of EP4 in HCs may induce an increase of intracellular cAMP levels, which activates the PKA pathway resulting in promotion of the HC survival. The regulation of growth factors such as vascular endothelial growth factor (VEGF) and hepatocyte growth factor (HGF) in the cochlea by EP4 agonists is also included in possible mechanisms for HC protection. Numerous previous reports have demonstrated that PGE increases VEGF expression (Bamba et al., 2000; Pai et al., 2001; Weiss et al., 2004) and HGF production (Makino et al., 2004; Zhang et al., 2000). Hatazawa (2007) demonstrated that $PGE_2$ stimulates VEGF expression through EP4 receptors. The upregulation of VEGF in the inner ear is involved in the recovery of auditory function after acoustic trauma, with potentially important clinical and therapeutic implications (Picciotti et al., 2006). HGF gene transfer to the subarachnoid space using virus vectors can prevent or ameliorate hearing impairment (Oshima et al., 2004). In addition, local

HGF protein application to the cochlea attenuates noise-induced damage on the cochlea (Inaoka et al., 2009). Such mechanisms might be involved in the EP4 agonist-induced protection of auditory HCs against injury caused by exposure to noise. The recovery of the circulation in the cochlea is also included in potential explanations for otoprotection by EP4 agonists. Local application of $PGE_2$ onto the RWM induces an increase of blood flow in the cochlea (Rhee et al., 1999). Exposure to intense noise causes reduction of the cochlear blood flow (Nakashima et al., 2003). Therefore, local EP4 treatment might improve a decrease of the cochlear blood flow due to noise exposure. Further studies are required to elucidate the detailed mechanisms underlying the EP4 agonist-induced protection of auditory HCs.

## CONCLUSION

The present findings demonstrate the expression of EP4 in the cochlea, and cochlear protection against noise trauma by local EP4 agonist application to the RWM. The elevation of the ABR threshold was significantly reduced, and histological analysis revealed that pre-treatment with an EP4 agonist significantly reduced the loss of OHCs. EP4 agonists might therefore have potential applications in clinical treatments against noise-induced hearing loss. However, the exact mechanisms by which EP4 agonists act in the cochlea are presently unclear and require further research.

*Acknowledgments—We thank Ono Pharmaceutical Co., Ltd. for providing ONO-AE1-329 and Dr. Yayoi S. Kikkawa for critically reviewing this work. This work was supported by a Grant-in-Aid for Researches on Sensory and Communicative Disorders from the Japanese Ministry of Health, Labour and Welfare.*

## REFERENCES

Ahmad AS, Ahmad M, de Brum-Fernandes AJ, Doré S (2005) Prostaglandin EP4 receptor agonist protects against acute neurotoxicity. Brain Res 1066:71–77.

Ahn JH, Kim MR, Kim HC (2005) Therapeutic effect of lipoprostaglandin E1 on sudden hearing loss. Am J Otolaryngol 26:245–248.

Alam SA, Robinson BK, Huang J, Green SH (2007) Prosurvival and proapoptotic intracellular signaling in rat spiral ganglion neurons in vivo after the loss of hair cells. J Comp Neurol 503:832–852.

Bamba H, Ota S, Kato A, Kawamoto C, Matsuzaki F (2000) Effect of prostaglandin $E_1$ on vascular endothelial growth factor production by human macrophages and colon cancer cells. J Exp Clin Cancer Res 19:219–223.

Bok J, Zha XM, Cho YS, Green SH (2003) An extranuclear locus of cAMP-dependent protein kinase action is necessary and sufficient for promotion of spiral ganglion neuronal survival by cAMP. J Neurol Sci 23:777–787.

Coleman RA, Smith WL, Narumiya S (1994) International union of pharmacology classification of prostanoid receptors: properties, distribution and structure of the receptors and their subtypes. Pharmacol Rev 46:205–229.

Echeverria V, Clerman A, Doré S (2005) Stimulation of PGE receptors EP2 and EP4 protects cultured neurons against oxidative stress and cell death following beta-amyloid exposure. Eur J Neurosci 22:2199–2206.

Hatazawa R, Tanigami M, Izumi N, Kamei K, Tanaka A, Takeuchi K (2007) Prostaglandin $E_2$ stimulates VEGF expression in primary rat gastric fibroblasts through EP4 receptors. Inflammopharmacology 15:214–217.

Inaoka T, Nakagawa T, Kikkawa YS, Tabata Y, Ono K, Yoshida M, Tsubouchi H, Ido A, Ito J (2009) Local application of hepatocyte growth factor using gelatin hydrogels attenuates noise-induced hearing loss in guinea pigs. Acta Otolaryngol 129:453–457.

Kabashima K, Saji T, Murata T, Nagamachi M, Matsuoka T, Segi E, Tsuboi K, Sugimoto Y, Kobayashi T, Miyachi Y, Ichikawa A, Narumiya S (2002) The prostaglandin receptor EP4 suppresses colitis, mucosal damage and CD4 cell activation in the gut. J Clin Invest 109:883–893.

Kataoka K, Takikawa Y, Lin SD, Suzuki K (2005) Prostaglandin $E_2$ receptor EP4 agonist induces Bcl-xL and independently activates proliferation signals in mouse primary hepatocytes. J Gastroenterol 40:610–616.

Kiriyama M, Ushikubi F, Kobayashi T, Hirata M, Sugimoto Y, Narumiya S (1997) Ligand binding specificities of the eight types and subtypes of the mouse prostanoid receptors expressed in Chinese hamster ovary cells. Br J Pharmacol 122:217–224.

Makino H, Aoki M, Hashiya N, Yamasaki K, Hiraoka K, Shimizu H, Azuma J, Kurinami H, Ogihara T, Morishita R (2004) Increase in peripheral blood flow by intravenous administration of prostaglandin $E_1$ in patients with peripheral arterial disease, accompanied by up-regulation of hepatocyte growth factor. Hypertens Res 27: 85–91.

Nakashima T, Naganawa S, Sone M, Tominaga M, Hayashi H, Yamamoto H, Liu X, Nuttall AL (2003) Disorders of cochlear blood flow. Brain Res Brain Res Rev 43:17–28.

Narumiya S, Sugimoto Y, Ushikubi F (1999) Prostanoid receptors: structures, properties, and functions. Physiol Rev 79:1193–1226.

Nitta M, Hirata I, Toshina K, Murano M, Maemura K, Hamamoto N, Sasaki S, Yamauchi H, Katsu K (2002) Expression of the EP4 prostaglandin $E_2$ receptor subtype with rat dextran sodium sulphate colitis: colitis suppression by a selective agonist, ONO-AE1-329. Scand J Immunol 56:66–75.

Ogawa K, Takei S, Inoue Y, Kanzaki J (2002) Effect of prostaglandin $E_1$ on idiopathic sudden sensorineural hearing loss: a double-blinded clinical study. Otol Neurotol 23:665–668.

Oshima K, Shimamura M, Mizuno S, Tamai K, Doi K, Morishita R, Nakamura T, Kubo T, Kaneda Y (2004) Intrathecal injection of HVJ-E containing HGF gene to cerebrospinal fluid can prevent and ameliorate hearing impairment in rats. FASEB J 18:212–214.

Pai R, Szabo IL, Soreghan BA, Atay S, Kawanaka H, Tarnawski AS (2001)PGE(2) stimulates VEGF expression in endothelial cells via ERK2/JNK1 signaling pathways. Biol Chem Biophys Res Commun 286: 923–928.

Picciotti PM, Fetoni AR, Paludetti G, Wolf FI, Torsello A, Troiani D, Ferraresi A, Pola R, Sergi B (2006) Vascular endothelial growth factor (VEGF) expression in noise-induced hearing loss. Hear Res 214:76–83.

Pujol R, Puel JL (1999) Excitotoxicity, synaptic repair, and functional recovery in the mammalian cochlea: a review of recent findings. Ann N Y Acad Sci 884:249–254.

Rhee CK, Park YS, Jung TT, Park CI (1999) Effects of leukotrienes and prostaglandins on cochlear blood flow in the chinchilla. Eur Arch Otorhinolaryngol 256:479–483.

Ruel J, Wang J, Rebillard G, Eybalin M, Lloyd R, Pujol R, Puel JL (2007) Physiology, pharmacology and plasticity at the inner hair cell synaptic complex. Hear Res 227:19–27.

Suzuki H, Fujimura T, Shiomori T, Ohbuchi T, Kitamura T, Hashida K, Udaka T (2008) Prostaglandin $E_1$ versus steroid in combination with hyperbaric oxygen therapy for idiopathic sudden sensorineural hearing loss. Auris Nasus Larynx 35:192–197.

Tominaga M, Yamamoto H, Sone M, Teranishi MA, Nakashima T (2006) Response of cochlear blood flow to prostaglandin $E_1$

applied topically to the round window. Acta Otolaryngol 126: 232–236.
Viberg A, Canlon B (2004) The guide to plotting a cochleogram. Hear Res 197:1–10.
Wei BP, Mubiru S, O'Leary S (2006) Steroids for idiopathic sudden sensorineural hearing loss. Cochrane Database Syst Rev 25: CD003998.
Weiss TW, Mehrabi MR, Kaun C, Zorn G, Kastl SP, Speidl WS, Pfaffenberger S, Rega G, Glogar HD, Maurer G, Pacher R, Huber K, Wojta J (2004) Prostaglandin $E_1$ induces vascular endothelial growth factor-1 in human adult cardiac myocytes but not in human adult cardiac fibroblasts via a cAMP-dependent mechanism. Mol Cell Cardiol 36:539–546.
Zhang L, Himi T, Murota S (2000) Induction of hepatocyte growth factor (HGF) in rat microglial cells by prostaglandin E(2). J Neurosci Res 62:389–395.
Zhuo XL, Wang Y, Zhuo WL, Zhang XY (2008) Is the application of prostaglandin $E_1$ effective for the treatment of sudden hearing loss? An evidence-based meta-analysis. J Int Med Res 36:467–470.

*(Accepted 8 March 2009)*
*(Available online 19 March 2009)*

*The Laryngoscope*


# Hepatocyte Growth Factor Protects Auditory Hair Cells From Aminoglycosides

Yayoi S. Kikkawa, MD, PhD; Takayuki Nakagawa, MD, PhD; Hirohito Tsubouchi, MD, PhD; Akio Ido, MD, PhD; Takatoshi Inaoka, MD; Kazuya Ono, MA; Juichi Ito, MD, PhD

**Objectives/Hypothesis:** To examine the effect of hepatocyte growth factor (HGF) for protection of auditory hair cells against aminoglycosides and its molecular mechanisms.

**Study Design:** Experimental study.

**Methods:** We quantitatively assessed protective effects of HGF on mouse cochlear hair cells against neomycin toxicity using explant culture systems. To understand mechanisms of hair cell protection by HGF, we examined the expression of c-Met, HGF receptor, and 4-hydroxynonenal (a lipid peroxidation marker) in the cochlea by means of immunohistochemistry and Western blotting.

**Results:** The application of HGF to cochlear explant cultures significantly reduced the hair cell loss induced by neomycin. Immunohistochemistry showed c-Met expression in normal auditory hair cells, and its increase in response to neomycin-induced damage. Immunostaining for 4-hydroxynonenal suggested that HGF acted by attenuating the lipid peroxidation of auditory epithelia induced by neomycin.

**Conclusions:** These findings demonstrate that a functional HGF/c-Met coupling is present in the cochlea, and HGF application exerts protective effects on hair cells, indicating the potential of HGF as a therapeutic agent for sensorineural hearing loss.

**Key Words:** Cochlea, protection, c-Met, growth factor, hearing loss, 4-hydroxynonenal.

***Laryngoscope*, 119:2027–2031, 2009**

From the Department of Otolaryngology–Head and Neck Surgery, Graduate School of Medicine, Kyoto University, Kyoto (Y.S.K., T.N., T.I., K.O., J.I.) and the Department of Digestive and Life-Style Related Diseases, Graduate School of Medical and Dental Sciences, Kagoshima University, Kagoshima (H.T., A.I.), Japan.

Editor's Note: This Manuscript was accepted for publication May 21, 2009.

This study was supported by a Grant-in-Aid for Special Purposes from the Ministry of Education, Science, Sports, Culture and Technology, and in part by a Grant-in-Aid for Researches on Sensory and Communicative Disorders from the Japanese Ministry of Health, Labor and Welfare of Japan.

Send correspondence to Takayuki Nakagawa, MD, PhD, Department of Otolaryngology–Head and Neck Surgery, Graduate School of Medicine, Kyoto University, Kawaharacho 54, Shogoin, Sakyo-ku, 606-8507 Kyoto, Japan. E-mail: tnakagawa@ent.kuhp.kyoto-u.ac.jp

**DOI: 10.1002/lary.20602**

## INTRODUCTION

Hepatocyte growth factor (HGF), which was initially identified and purified as a multifunctional protein in hepatocytes,[1] exerts its activities, such as mitogenic, morphogenic, angiogenic, and antiapoptotic activities, in various types of cells,[2,3] including neuronal cells. HGF, and its receptor c-Met, are expressed in various regions of the brain and peripheral neurons.[2–4] A functional coupling between HGF and c-Met has been reported to play important roles in the development and the maintenance of the nervous system.[5,6] Previous studies have revealed that HGF gene transfer with hemagglutinating virus of Japan envelope (HVJ-E) prevents postischemic delayed neuronal death in the hippocampus.[2,7] Kitamura et al. also delivered the HGF gene to the injured spinal cords using herpes simplex virus-1.[8] Altogether, these studies suggest that HGF functions as a neurotrophic factor to maintain the physiological structure and function of the nervous system.

Several studies indicated a therapeutic potential of HGF for inner ear disorders. Previously, Oshima et al. reported that HGF gene delivery into the cerebrospinal fluid with HVJ-E vector promotes functional recovery after aminoglycoside-induced hearing loss.[9] Recently, we have demonstrated that local application of recombinant human HGF protein into the cochlea using gelatin hydrogels,[10] which enables sustained delivery of growth factors, rescues auditory hair cells from noise-induced damage.

However, actual mechanism of HGF action to the hair cells is not yet clearly described. The present study aimed to explore the molecular mechanism of HGF effect and examine the potential of HGF. We used cochlear explant culture systems and tested the capability of HGF for protection of auditory hair cells against aminoglycoside toxicity. In addition, to explore the HGF signaling mechanism on the auditory epithelium, we examined the expression of the c-Met receptor and monitored the changes in lipid oxidation in auditory epithelia damaged by neomycin.

## MATERIALS AND METHODS

### *Animals*

ICR mice (Japan SLC, Hamamatsu, Japan) were used in this study. The Animal Research Committee, Graduate School

of Medicine, Kyoto University, approved all experimental protocols. Animal care was under the supervision of the Institute of Laboratory Animals, Graduate School of Medicine, Kyoto University. All experimental procedures were performed in accordance with the *NIH Guide for the Care and Use of Laboratory Animals*.

### *Cochlear Explant Culture*

On postnatal day 3 (P3), ICR mice were deeply anesthetized with sevoflurane and decapitated. The temporal bones were dissected, and the cochleae were freed from surrounding tissues in 0.01 M phosphate-buffered saline (PBS) at pH 7.4. After removal of the cochlear lateral wall, auditory epithelia were dissected from the cochlear modiolus. The tissue pieces were then attached to glass mesh inserts (Falcon, Billerica, MA) and cultured initially in serum-free minimum essential medium (Invitrogen, Eugene, OR) supplemented with 3 g/L glucose and penicillin G for 24 hours. Cultures were incubated at 37°C in a humidified atmosphere of 95% air and 5% $CO_2$. Because hair cells in the apex are resistant to aminoglycosides,[11,12] basal turns of the cochlea were used in this study.

### *Neomycin Application, Cell Survival, and HGF Protection Assay*

The explants were then transferred to the medium containing neomycin sulfate (Sigma-Aldrich, St. Louis, MO) at concentrations of 0, 0.1, 0.3, 1, or 3 mM, with six to 10 cochleae incubated at each concentration. For HGF protection assay, we examined effects of 20 ng/mL recombinant human HGF (rhHGF, Sigma-Aldrich) with the same neomycin concentrations. We also used 1 mM neomycin media supplemented with recombinant human HGF at concentrations of 0, 4, 20, or 100 ng/mL to estimate optimal HGF concentration.

Cultures were maintained for 24 hours and at the end of the culture period, samples were fixed for 15 minutes in 4% paraformaldehyde in 0.1 M phosphate buffer (pH 7.4). Specimens were then rinsed with PBS, incubated in 1% bovine serum albumin (BSA) with 0.2% Triton X-100 for 30 minutes and immersed in Alexa 488-labeled phalloidin (1:200; Invitrogen) for 30 minutes. Samples were examined with a Leica TCS-SP2 confocal microscope (Leica Microsystems Inc., Wetzlar, Germany). To quantify hair cell loss in the cochlea after various treatments, inner hair cells (IHCs) and outer hair cells (OHCs) in the auditory epithelia were counted over a 100-$\mu$m longitudinal distance from two separate regions in the basal turn of each culture (totaling 200 $\mu$m).

### *c-Met Expression in the Cochlea*

Temporal bones of P3 ICR mice (n = 4) were collected under deep anesthesia. Cochleae were perfused with saline followed by 4% paraformaldehyde in 0.1 M phosphate buffer and immersed in the same fixative at room temperature for 2 hours. After ethylenediaminetetraacetic acid decalcification, the specimens were embedded in optimum cutting temperature compound (Tissue Tek, Miles Inc., Elkhart, IN) and sectioned at 15 $\mu$m using a cryostat. Midmodiolar sections were provided for immunohistochemistry. Sections were briefly refixed with 4% paraformaldehyde and blocked with 1% BSA with 0.2% Triton X-100 for 30 minutes. Primary antibodies were rabbit polyclonal anti-c-Met (1:100, Santa Cruz Biotechnology, Santa Cruz, CA) and anti-myosin VIIa (1:500, Proteus Bioscience Inc., Ramona, CA). Alexa-Fluor 488-conjugated goat anti-rabbit IgG (1:200; Invitrogen) were used as the secondary antibody, and Zenon Alexa Fluor 555 rabbit IgG labeling kit (Invitrogen) was used for anti-myosin VIIa staining. Specimens were then incubated in PBS containing 2 mg/mL DAPI (Invitrogen) for nuclear staining.

### *Alteration of c-Met Levels in Cochlear Explants*

We employed Western blotting to estimate alterations of c-Met expression in cochlea explants following neomycin application. Cochlear explants were cultured without glass mesh, using medium containing neomycin sulfate at concentrations of 0, 0.3, 1, or 3 mM for 24 hours. Ten cochleae were used for each condition. Explants were then quickly collected and homogenated in ice-cold radio immunoprecipitation assay buffer with protease inhibitor cocktail (Nakalai Tesque, Kyoto, Japan). Five micrograms of each extract was separated on a 4% to 15% Tris-HCL gradient polyacrylamide gel (Bio-Rad, Hercules, CA) and then transferred to a polyvinylidene fluoride membrane (Millipore, Billerica, MA). Membranes were blocked for 40 minutes with 5% BSA in Tween-TBS (10 mM Tris-HCl pH 7.5, 150 mM NaCl, 0.05% Tween 20) and stained overnight with anti-c-Met antibody or antiactin antibody (Sigma) at 4°C. After three washes the membranes were incubated in a 1:20000 dilution of horseradish peroxidase-conjugated secondary antibody for 1 hour and developed using the ECL plus Western blotting detection system (Amersham Pharmacia Biotech, Uppsala, Sweden). Experiments were repeated three times and pictures were processed with Adobe Photoshop CS (Adobe Systems, San Jose, CA), and band intensity was measured using ImageJ software (http://rsb.info.nih.gov/ij/; National Institutes of Health, Bethesda, MD).

### *Lipid Peroxidation Assay*

Lipid peroxidation was assessed in cultures treated with neomycin, in the presence or absence of HGF, by measuring expression of 4-hydroxynonenal (HNE) immunohistochemically.[13] Explants were labeled with mouse anti-HNE monoclonal antibody (1:8; Oxis Research, Portland, OR) and Alexa-Fluor 568 goat anti-mouse IgG (1:200; Invitrogen) as the primary and secondary antibodies. Specimens were then counterstained with Alexa 488 phalloidin and examined with a fluorescence microscope. All images were taken with the same exposure and shutter speed. Red fluorescence intensity was measured using ImageJ software.

### *Statistical Analysis*

Overall effects of HGF on hair cell numbers were analyzed by 2-way factorial analysis of variance (ANOVA) using the Statcel2 application (OMS Publishing, Saitama, Japan), with *P* values below .05 considered statistically significant. For interactions that were significant, multiple paired comparisons were analyzed using the Tukey-Kramer test. Measurements of HNE staining intensity were analyzed with 1-way ANOVA with the Tukey-Kramer test.

## RESULTS

### *Dose-Dependent Hair Cell Loss by Neomycin*

First, we tested a dose-response relationship between neomycin concentrations and hair cell counts. The addition of 0-3 mM neomycin for 24 hours significantly reduced hair cell numbers in both IHC and OHC regions (Fig. 1A, C, E, G). The addition of 1 mM of neomycin destroyed approximately 73% of the IHCs and 64% of the OHCs (Fig. 1E, I). The hair cell density

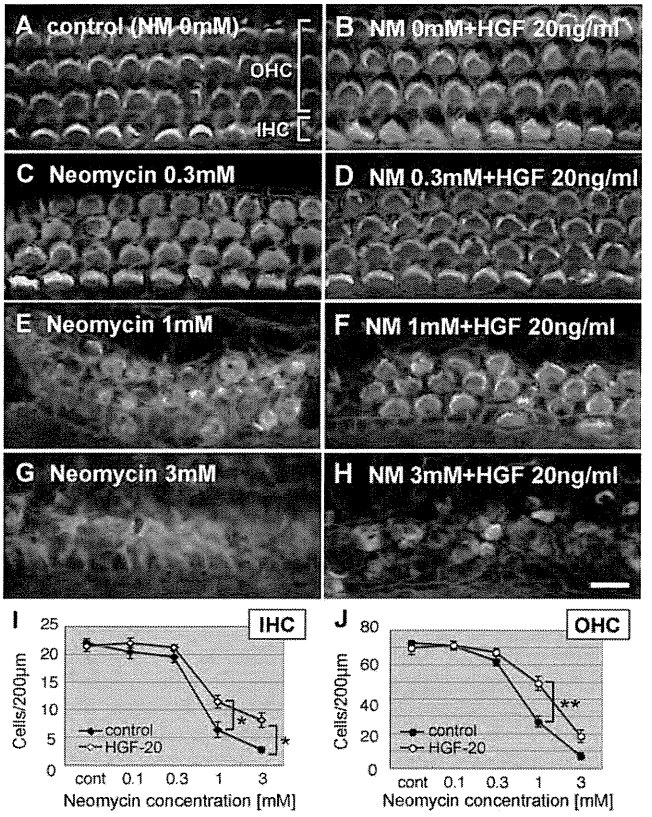


Fig. 1. Dose-dependent auditory hair cell loss by neomycin and its protection by hepatocyte growth factor (HGF). Cochleae were cultured for 24 hours in various concentrations of neomycin with or without HGF. (A–H). Photomicrographs of phalloidin-labeled cochlear cultures. Outer hair cell (OHC) consists of three rows of triangular-shaped cells that have phalloidin-positive, inverted v-shaped stereocilia bundles on top of them. Inner hair cells (IHC) are oval-shaped cells that have flat, u-shaped stereocilia bundles. Bar = 10 $\mu$m. (A). A control showing normal arrangement of IHCs and OHCs. (C, E, G). Examples of cochlear cultures treated with neomycin at a concentration of 0.3 mM (C), 1 mM (E), and 3 mM (G). (B, D, F, H). Examples of cochlear cultures treated with 20 ng/mL HGF and neomycin at a concentration of 0 mM (B), 0.3 mM (D), 1 mM (F), and 3 mM (H). (I, J). Hair cell count following neomycin and HGF-supplemented cultures. Filled symbols represent counts from control cultures without HGF and open symbols from HGF- supplemented cultures. In HGF-free cultures, the hair cell density decreased systematically as the neomycin concentration increased. HGF significantly attenuated the loss of IHC ($P < .05$) and OHC ($P < .001$) in neomycin-damaged cochleae (2-way analysis of variance). Post hoc analyses with Tukey-Kramer tests for multiple pairwise comparisons showed that IHC loss for HGF plus neomycin was significantly less ($P < .05$) than for neomycin alone at neomycin concentrations of 1 and 3 mM, and also enhanced the survival of OHCs at 1 mM neomycin ($P < .01$). *$P < .05$. **$P < .01$. Bars in (I) and (J) represent standard errors.

decreased as the neomycin dose increased until virtually all hair cells were absent from the auditory epithelium cultured in 3 mM neomycin.

### *Dose-Response Effects of HGF Against Neomycin*

To assess whether HGF has protective effects against neomycin damage, we examined the power of HGF on a quantitative assessment of dose-response relationship of the hair cells to various concentrations of neomycin. We administered 20 ng/mL HGF to 0, 0.1, 0.3, 1, or 3 mM neomycin cultures (Fig. 1B, D, F, H). The addition of 20 ng/mL HGF markedly enhanced IHC and OHC survival. HGF even promoted the survival of a substantial number of hair cells at the highest neomycin dose, 3 mM (Fig. 1G vs. H). Two-way ANOVA analyses showed that HGF has a significant effect on both remaining IHC and OHC numbers ($P = .000097$ and $P = .0000011$, respectively). Tukey-Kramer tests for multiple pairwise comparisons showed that IHC losses for HGF at 1 or 3 mM neomycin was significantly less ($P < .05$) than those for neomycin alone conditions (Fig. 1I). Twenty ng/mL HGF also significantly ($P < .01$) enhanced the survival of OHCs at 1 mM neomycin condition (Fig. 1J). These data demonstrated that HGF exerts significant protective effects against neomycin-induced hair cell damage.

### *Optimal Concentration of HGF for Protection*

We then administered 4 to 100 ng/mL HGF to these cultures (Fig. 2). Based on the above dose-response experiment, 1 mM neomycin was used. When HGF was administered alone to control cultures at 4 to 100 ng/mL, the number of hair cells present in the samples was comparable to untreated controls indicating that HGF alone had no negative or mitogenic effects at these concentrations (Fig. 1B). In neomycin-

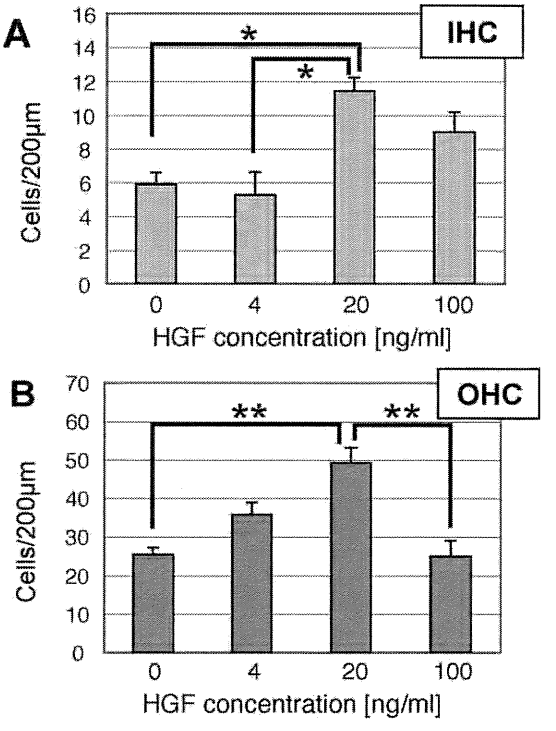


Fig. 2. Effects of different concentrations of hepatocyte growth factor (HGF) on the survival of cochlear hair cells. Cochleae were incubated with different concentrations of HGF in the presence of 1 mM neomycin. (A) Inner hair cell (IHC) and (B) outer hair cell (OHC) counts in HGF-treated cultures. HGF significantly increased hair cell survival at concentrations up to 20 ng/mL. *$P < .05$. **$P < .01$. Bars represent standard errors.

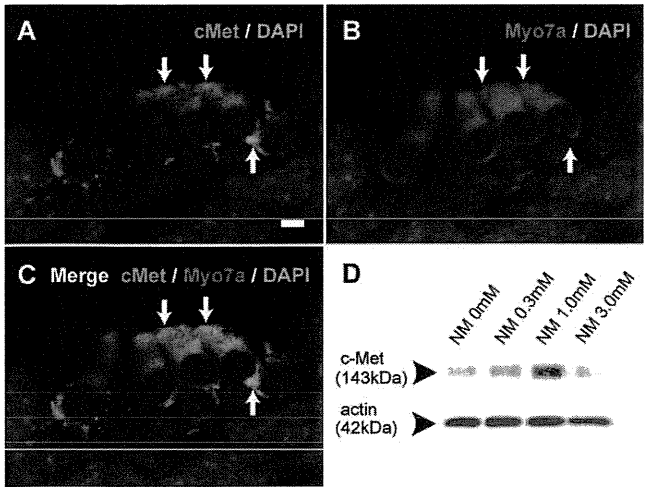


Fig. 3. c-Met expression in the organ of Corti increases after neomycin insult. (A, B, C). c-Met localization (green) in a normal postnatal day 3 cochlea. Specimen was counterstained with anti-myosin VIIa (red) and DAPI (blue). Arrows indicate punctuate c-Met staining in the hair cells. Bar = 10 $\mu$m. (D). Induction of c-Met expression in the neomycin-injured cochlea. Western blotting analyses showed a remarkable increase of c-Met expression, peaking when neomycin was applied at 1.0 mM. Relative band intensities were 1.00, 1.12 $\pm$ 0.26, 1.94 $\pm$ 0.48, and 1.17 $\pm$ 0.35 for 0, 0.3, 1.0, and 3.0 mM neomycin (n = 10 in each condition).

supplemented cultures, adding 4 ng/mL of HGF had little effect on IHC survival. In comparison, HGF treatment at 20 ng/mL elicited 64% increase of remaining cell counts. However, at concentration of 100 ng/mL HGF, no further increases in the number of IHCs were seen, indicating that HGF effects saturated at 20 ng/mL concentration. A 1-way ANOVA revealed significant treatment effects for HGF ($P = .018$). Tukey-Kramer tests for multiple pairwise comparisons showed significant differences between the 0 and 20 ng/mL neomycin ($P < .05$) and 4 and 20 ng/mL neomycin groups ($P < .05$). HGF had similar effects on OHC survival (Fig. 2B). HGF treatment at 20 ng/mL elicited almost a two-fold increase of remaining cell counts. A 1-way ANOVA revealed significant effects for HGF ($P = .000049$). Tukey-Kramer tests for multiple pairwise comparisons showed significant differences between the 0 and 20 ng/mL neomycin ($P < .01$) and 20 and 100 ng/mL neomycin groups ($P < .01$). Based on these findings, the optimal concentration of HGF to 1 mM neomycin damage was estimated as 20 ng/mL for both IHCs and OHCs.

### *c-Met Localization in the Auditory Epithelia*

To reveal whether cochlear protection mechanism of HGF is mediated by HGF/c-Met paracrine coupling, we first examined c-Met expression in the cochlea using immunohistochemistry (Fig. 3A, B, C). The expression of c-Met was detected punctate in both IHCs and OHCs, most densely at the apical region of the OHCs and the nerve ending (basal) area of IHCs and OHCs. In contrast, surrounding supporting cells expressed minimal amount of c-Met.

### *c-Met Expression Increases After Neomycin Insult*

We then tested whether neomycin damage could increase c-Met expression in the hair cells. We examined c-Met expression in cochlear explant cultures after 24 hours of 0 to 3 mM neomycin application. Western blotting revealed that c-Met expression peaked when neomycin was applied at 1.0 mM (Fig. 3D). Relative band intensity was 1.94 $\pm$ 0.48 compared to that of 0 mM neomycin. At 3.0 mM neomycin, band intensity decreases, corresponding to fewer hair cells remaining in the auditory epithelia at this neomycin concentration (Fig. 1G).

### *Antioxidant Effects of HGF*

We also investigated the antioxidant effect of HGF, as another mechanism by which its protective effect might function. HNE expression in explant cultures increased in the presence of neomycin (Fig. 4). Adding HGF to the cultures resulted in a significant reduction in HNE expression ($P = .00049$). HGF showed its greatest effect at a concentration of 4 ng/mL, at which HNE production was attenuated to 59.0% of the level in the absence of HGF.

## DISCUSSION

The present study has demonstrated that the application of HGF attenuates neomycin-induced hair cell death in cochlear explants. In our experimental setting, quantitative assessments of hair cell numbers following neomycin application exhibits that both IHC and OHC numbers decrease as the neomycin dose increases. In this setting we examined the effects of 20 ng/mL HGF and the results demonstrated significant effects of HGF on dose-dependent hair cell loss by neomycin, which strongly supports our hypothesis that HGF is a potent protectant for the cochlear hair cells. Also, in using a concentration of 1 mM neomycin, which provides a significant lesion to the hair cells, we showed that the optimal concentration of HGF is 20 ng/mL for hair cell protection in explant cultures.

HGF protection of neuronal cells is believed to involve various mechanisms including HGF/c-Met

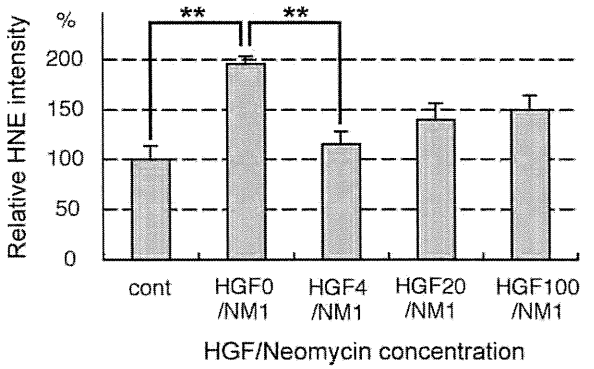


Fig. 4. Hepatocyte growth factor (HGF) treatment reduced lipid oxygenation. Lipid oxygenation was measured in cultures treated with neomycin and HGF as the intensity of immunohistochemical labeling for 4-hydroxynonenal (HNE). Relative HNE staining intensity in the organ of Corti was significantly increased in the presence of 1 mM neomycin, but significantly reduced with the addition of 4 ng/mL HGF. **$P < .01$. Bars represent standard errors.

signaling.[5,6] We thus investigated involvement of HGF/c-Met signaling in hair cell protection by HGF against neomycin toxicity. Immunohistochemistry in normal P3 mouse cochleae revealed the presence of c-Met in cochlear hair cells. In addition, Western blotting demonstrated an increase of c-Met expression after neomycin-induced damage. These findings indicate involvement of paracrine coupling between HGF and c-Met in the auditory epithelium and the central nervous system.[5] Also, the increase of c-Met expression after neomycin-induced damage justifies exogenous HGF application for hair cell protection.

HGF could also protect hair cells from damage by reducing the oxidative stress generated by neomycin. Several researchers have reported that HGF exerts antioxidant activity by enhancing reactive oxygen species (ROS) scavenging and suppressing ROS production.[14,15] We have previously shown that lipid peroxidation caused by hydroxyl radicals increases in the auditory epithelium during cisplatin-induced hearing trauma.[13] In this study, our results indicated that lipid peroxidation also occurred in the neomycin-damaged cochlea, and HGF successfully attenuated HNE expression at a concentration of 4 ng/mL. We therefore consider that the antioxidant activity of HGF may in part play a role in the mechanisms by which it protects hair cells.

## CONCLUSION

We have provided evidence for the direct survival-promoting effect of HGF on cochlear hair cells. Our data indicate that damaged auditory epithelia express c-Met receptors and HGF is a candidate as a delivering drug to the cochlea for treatment of sensorineural hearing loss.


### Acknowledgments

We thank all Kyoto University otology lab members for critical review of the manuscript and Ms. Keiko Nishio for secretarial assistance.


## BIBLIOGRAPHY


1. Gohda E, Tsubouchi H, Nakayama H, et al. Purification and partial characterization of hepatocyte growth factor from plasma of a patient with fulminant hepatic failure. *J Clin Invest* 1988;81:414–419.
2. Miyazawa T, Matsumoto K, Ohmichi H, Katoh H, Yamashima T, Nakamura T. Protection of hippocampal neurons from ischemia-induced delayed neuronal death by hepatocyte growth factor: a novel neurotrophic factor. *J Cereb Blood Flow Metab* 1998;18: 345–348.
3. Funakoshi H, Nakamura T. Hepatocyte growth factor: from diagnosis to clinical applications. *Clin Chim Acta* 2003; 327:1–23.
4. Yamada T, Tsubouchi H, Daikuhara Y, et al. Immunohistochemistry with antibodies to hepatocyte growth factor and its receptor protein (c-MET) in human brain tissues. *Brain Res* 1994;637:308–312.
5. Honda S, Kagoshima M, Wanaka A, Tohyama M, Matsumoto K, Nakamura T. Localization and functional coupling of HGF and c-Met/HGF receptor in rat brain: implication as neurotrophic factor. *Brain Res Mol Brain Res* 1995;32:197–210.
6. Maina F, Pante G, Helmbacher F, et al. Coupling Met to specific pathways results in distinct developmental outcomes. *Mol Cell* 2001;7:1293–1306.
7. Hayashi K, Morishita R, Nakagami H, et al. Gene therapy for preventing neuronal death using hepatocyte growth factor: in vivo gene transfer of HGF to subarachnoid space prevents delayed neuronal death in gerbil hippocampal CA1 neurons. *Gene Ther* 2001;8: 1167–1173.
8. Kitamura K, Iwanami A, Nakamura M, et al. Hepatocyte growth factor promotes endogenous repair and functional recovery after spinal cord injury. *J Neurosci Res* 2007;85: 2332–2342.
9. Oshima K, Shimamura M, Mizuno S, et al. Intrathecal injection of HVJ-E containing HGF gene to cerebrospinal fluid can prevent and ameliorate hearing impairment in rats. *FASEB J* 2004;18:212–214.
10. Inaoka T, Nakagawa T, Kikkawa Y, et al. Local application of hepatocyte growth factor using gelatin hydrogels attenuates noise-induced hearing loss in guinea pigs. *Acta Otolaryngol* 2009;129:453–457.
11. Romand R, Chardin S. Effects of growth factors on the hair cells after ototoxic treatment of the neonatal mammalian cochlea in vitro. *Brain Res* 1999;825:46–58.
12. Kopke R, Allen KA, Henderson D, Hoffer M, Frenz D, Van de Water T. A radical demise. Toxins and trauma share common pathways in hair cell death. *Ann N Y Acad Sci* 1999;884:171–191.
13. Lee JE, Nakagawa T, Kim TS, et al. Role of reactive radicals in degeneration of the auditory system of mice following cisplatin treatment. *Acta Otolaryngol* 2004;124: 1131–1135.
14. Li H, Jiang T, Lin Y, Zhao Z, Zhang N. HGF protects rat mesangial cells from high-glucose-mediated oxidative stress. *Am J Nephrol* 2006;26:519–530.
15. Jin M, Yaung J, Kannan R, He S, Ryan SJ, Hinton DR. Hepatocyte growth factor protects RPE cells from apoptosis induced by glutathione depletion. *Invest Ophthalmol Vis Sci* 2005;46:4311–4319.

Molecular and Cellular Neuroscience 42 (2009) 391–398

Contents lists available at ScienceDirect

Molecular and Cellular Neuroscience

journal homepage: www.elsevier.com/locate/ymcne

# Silencing p27 reverses post-mitotic state of supporting cells in neonatal mouse cochleae

Kazuya Ono [a], Takayuki Nakagawa [a,*], Ken Kojima [a], Masahiro Matsumoto [a], Takeshi Kawauchi [b], Mikio Hoshino [c], Juichi Ito [a]

[a] Department of Otolaryngology, Head and Neck Surgery, Graduate School of Medicine, Kyoto University, Kawaharacho 54, Shogoin, Sakyo-ku, 606-8507 Kyoto, Japan
[b] Department of Anatomy, Keio University School of Medicine, 160-8582 Tokyo, Japan
[c] Department of Biochemistry and Cellular Biology, National Institute of Neuroscience, National Center of Neurology and Psychiatry, 187-8502 Tokyo, Japan

ARTICLE INFO

*Article history:*
Received 8 May 2009
Revised 30 July 2009
Accepted 30 August 2009
Available online 4 September 2009

*Keywords:*
RNA interference
Cyclin-dependent kinase inhibitor
Cochlea
Mitosis
Apoptosis
Regeneration

ABSTRACT

The post-natal cochlear mammalian epithelium have no capacity to proliferate in tissue, however, dissociated supporting cells exhibit the ability to divide and trans-differentiate into new hair cells *in vitro*, with this process found to be correlated with the downregulation of the cyclin-dependent kinase inhibitor $p27^{kip1}$. Here we show that knockdown of $p27^{kip1}$ with short hairpin RNA-expressing vectors results in the cell-cycle reentry of post-mitotic supporting cells in the post-natal mouse cochleae *ex vivo*. The $p27^{kip1}$-knockdown cells incorporated BrdU, and then divided into two daughter cells. However, there was also activation of the apoptotic pathway in some supporting cells. These results indicate that the use of RNA interference to target *$p27^{kip1}$* is an effective strategy for inducing cell-cycle reentry in post-mitotic supporting cells in the post-natal mammalian cochleae, although additional manipulations of the supporting cells are required to achieve hair cell regeneration.



## Introduction

Sensorineural hearing loss (SNHL) is one of the most common disabilities. Auditory hair cells in the cochlea are mechanoreceptors that play a crucial role in hearing. In mammals, if the hair cells are damaged or lost, the resulting SNHL is permanent. Therefore, one of the best approaches for improving hearing in mammals would be to find a way to induce hair cell regeneration.

The cochlear epithelium is composed of hair cells and supporting cells (SCs). In the avian auditory epithelium, SCs are able to reenter the cell cycle and proliferate in response to hair cell loss, which gives rise to both new hair cells and SCs (Corwin and Cotanche, 1988; Ryals and Rubel, 1988). In mice, progenitors of the cochlear epithelium stop dividing by embryonic day 14.5 (Ruben, 1967), with differentiation of the hair cells and SCs occurring after this terminal mitosis. Both hair cells and SCs maintain a post-mitotic state throughout life in adult mammals, and do not exhibit any spontaneous capacity to divide under normal conditions or in response to damage *in vivo* (Roberson and Rubel, 1994).

It has been determined that the cyclin-dependent kinase inhibitor (CKI), $p27^{kip1}$, plays a crucial role in the entry of mammalian SCs into the G0 phase (Chen and Segil, 1999; Löwenheim et al., 1999). CKIs function by binding to and inhibiting the activity of the cyclin-dependent kinases that promote cell cycle progression and fulfill the cell cycle checkpoint functions (Sherr and Roberts, 1999). The $p27^{kip1}$ acts as a negative regulator of the G1-S transition in the cell cycle (Harper, 2001). Studies on $p27^{kip1}$-deficient mice have shown that when deleted, it results in the continued proliferation of SCs in postnatal mouse cochlear epithelia (Chen and Segil, 1999; Löwenheim et al., 1999). Recently, White et al. (2006) have reported that after dissociation, some of the mammalian SCs are able to recover their proliferative abilities. In addition, these dissociated SCs can also trans-differentiate into hair cells *in vitro*. These findings suggest that while these mammalian SCs might have a regenerative potential similar to avian auditory epithelia, this potential is suppressed within the tissue. This previous study also found that there was a correlation between the reduced expression levels of $p27^{kip1}$ and the ability of the mammalian supporting cells to reenter the cell cycle *in vitro*. Overall, these previous results suggest that manipulation of the $p27^{kip1}$ levels could be used therapeutically to stimulate the proliferation of mammalian SCs in tissue.

Discovery of gene inactivation by RNA interference (RNAi) has led to the development of a new targeted therapy for inner ear disease at the molecular level (Fire et al., 1998). RNAi is a two-stage intracellular process that converts the double-stranded RNA molecule precursors into functional small interfering RNAs. These small interfering RNAs are then incorporated into RNA-inducing silencing complexes. Subsequently, these duplexes unwind, with one strand used to target sequence-specific cleavage of the messenger RNAs that ultimately cause the knockdown of the expression of the targeted proteins (Elbashir et al., 2001).

* Corresponding author. Fax: +81 75 751 7225.
*E-mail address:* tnakagawa@ent.kuhp.kyoto-u.ac.jp (T. Nakagawa).

1044-7431/$ – see front matter © 2009 Elsevier Inc. All rights reserved.
doi:10.1016/j.mcn.2009.08.011

Although studies on p27$^{kip1}$-deficient mice have shown that its deletion results in continued SC proliferation in postnatal mouse cochlear epithelia (Chen and Segil, 1999; Löwenheim et al., 1999), the consequences of acute removal of p27$^{kip1}$ from differentiated SCs have yet to be examined. Therefore, the aim of the current study was to examine the efficacy of RNAi in silencing p27$^{kip1}$ in cochlear explant cultures from post-natal mice, and its potential for inducing mitosis in post-mitotic SCs in the cochlear epithelia after birth.

## Results and discussion

### *Co-transfection efficiency*

In this study, the two different plasmids were simultaneously introduced into the cochlear explants in order to label cells in which short hairpin RNAs (shRNAs) were transfected. To examine the efficiency of co-transfection, we introduced two different plasmids, EGFP- and DsRed-expressing vectors, into five cochlear explants via electroporation. One day after the electroporation, EGFP+ cells were found in all explants, with the majority co-expressing DsRed (Fig. 1a, b). Immunostaining for p27$^{kip1}$ identified SCs within the cochlear epithelia (Fig. 1c). DsRed was expressed in $32.5 \pm 11.0/33.0 \pm 10.9$ EGFP+, p27$^{kip1}$+ cells (98.5%), and there were $32.5 \pm 11.0/33.5 \pm 12.4$ DsRed+, p27$^{kip1}$+ cells (97.0%) that expressed EGFP. These results demonstrated that electroporation was able to simultaneously introduce two different plasmids into the SCs.

### *Silencing p27$^{kip1}$ expression in SCs by RNAi*

ShRNA for p27$^{kip1}$-expressing vectors, sh-p27a, or the control scrambled shRNA vector, sh-scr, were co-electroporated with pEGFP-N1 into cochlear explants ($n = 5$ in each condition). Two days after the introduction of a mixture of sh-scr and pEGFPN-1, $48.4 \pm 13.7$ EGFP-expressing cells were found in the *whole single* cochlear explant, with all the EGFP-expressing cells positive for p27$^{kip1}$ (Fig. 2g–h'). These results indicate that transfection of plasmids into SCs did occur and that there was no silencing of the expression of p27$^{kip1}$. In sh-p27a-transfected explants, $28.4 \pm 7.8/29.7 \pm 7.7$ EGFP-expressing cells (95.4%) exhibited no expression of p27$^{kip1}$ (Fig. 2i–l), indicating that silencing of the expression of p27$^{kip1}$ occurred in these SCs.

To confirm that EGFP+ and p27$^{kip1}$-cells were SCs after the knockdown of p27$^{kip1}$, we performed immunostaining for myosin VIIa and Sox2 in explants in which sh-p27a has been introduced. Cochlear specimens of post-natal day 3 (P3) mice 1 day *in vitro* were used as the immunohistochemistry controls. In controls, immunostaining for myosin VIIa and p27$^{kip1}$ clearly demonstrated the location of the hair cells (Fig. 2a, d), and the p27$^{kip1}$–labeled SC layer (Fig. 2b, e), which was located underneath the hair cell layer. Sox2 was strongly expressed in the SCs in the organ of Corti and in the inner sulcus region (which corresponds to the interior of the organ of Corti), but in the outer sulcus region (which corresponds to the exterior of the organ of Corti), it was either faintly seen or not found at all within the SCs (Fig. 2c, f), which is identical to previous findings (Oesterle et al., 2008; Hume et al., 2007). In sh-p27a-transfected specimens ($n = 5$), double labeling for myosin VIIa and p27$^{kip1}$ demonstrated that the EGFP+ and p27$^{kip1}$-cells were located underneath the myosin VIIa+ hair cell layer (Fig. 2i'), which was coincident with the location of the SCs. Double labeling for Sox2 and p27$^{kip1}$ demonstrated that all EGFP+ and p27$^{kip1}$- cells that were located in the organ of Corti (41 cells in four explants) were positive for Sox2 (Fig. 2k-m). Overall, these results demonstrated that the introduction of sh-p27 efficiently silenced p27$^{kip1}$ expression in the SCs.

In addition, to examine the efficacy of transfection in pillar cells and Deiters' cells, immunostaining for Prox1 was performed (Kirjavainen et al., 2008). In P3 mouse cochleae, the expression of Prox1 was found in pillar cells and Deiters' cells (Fig. 3a). In sh-p27a-transfected specimens ($n = 7$), a few EGFP+ Prox1+ cells were found (Fig. 3b–d). The mean was $2.1 \pm 1.9$ cells in the whole single cochlea, which is $4.4 \pm 3.5\%$ of total EGFP+ cells in the whole single cochlea. Other EGFP-expressing cells were located in the outer sulcus region. In the inner sulcus region, no EGFP-expressing cells were found.

### *S-phase reentry of SCs by silencing p27$^{kip1}$*

To examine whether p27$^{kip1}$ silencing had an effect on the reentry of SCs into the cell cycle, a 5-bromo-2-deoxyuridine (BrdU)-labeling assay was employed. To confirm that the S-phase reentry of the SCs is specific to the knockdown of p27$^{kip1}$, we used two different shRNAs to target p27$^{kip1}$ in this experiment. Explants after introduction of the plasmid mixtures, pEGFP-N1 and, sh-p27a ($n = 9$), sh-p27b ($n = 5$) or sh-scr ($n = 5$) were used. Three days after the introduction of a mixture of sh-scr and pEGFPN-1, there were no double-positive BrdU+ EGFP+ cells seen in the cochlear epithelia (Fig. 4a–d). While we found that a few mesenchymal cells located under the basement membrane of the cochlear epithelium were positive for BrdU, all of these were found to be negative for EGFP (Fig. 4a'–d'). In an explant transfected with sh-p27a, $13.8 \pm 6.8/48.2 \pm 15.2$ EGFP+ cells (28.6%) were labeled by BrdU with no expression of p27$^{kip1}$ (Fig. 4e–h'). In cochlear explants transfected with sh-p27b, BrdU+, EGFP+ cells were also found in the cochlear epithelia (Fig. 4i-l'). BrdU incorporation was identified in $7.6 \pm 4.7/24.6 \pm 15.0$ EGFP+ cells (30.9%). These results demonstrated that silencing p27$^{kip1}$ expression occurred after transfection of shRNA that was directed against *p27$^{kip1}$* and led to the initiation of S-phase reentry of the post-mitotic SCs. However, the knockdown of p27$^{kip1}$ did not induce S-phase reentry in approximately 70% of transfected cells. There are two possible

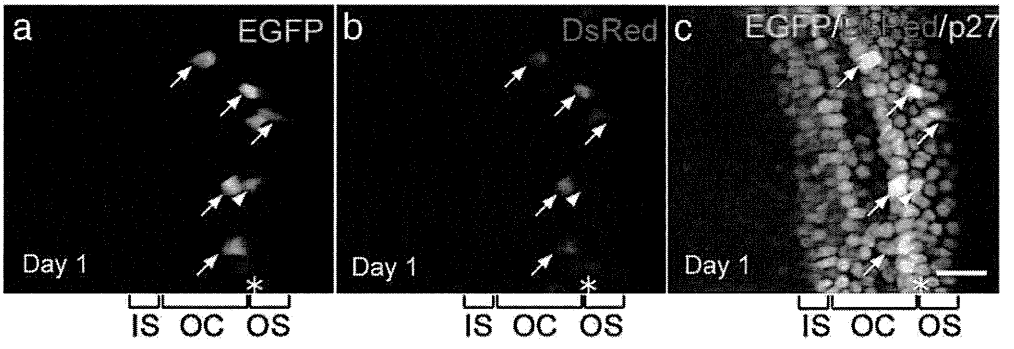


**Fig. 1.** Electroporation-mediated co-transfection of two different plasmids into cochlear supporting cells. Co-expression of EGFP (a) and DsRed (b) are found in supporting cells, which is identified by p27$^{kip1}$ immunostaining (c) 1 day after electroporation (arrows). An arrowhead indicates an EGFP+, DsRed- cell, and an asterisk shows an EGFP-, DsRed+ cell. IS, inner sulcus; OC, organ of Corti; OS, outer sulcus. Scale bar = 30 μm.

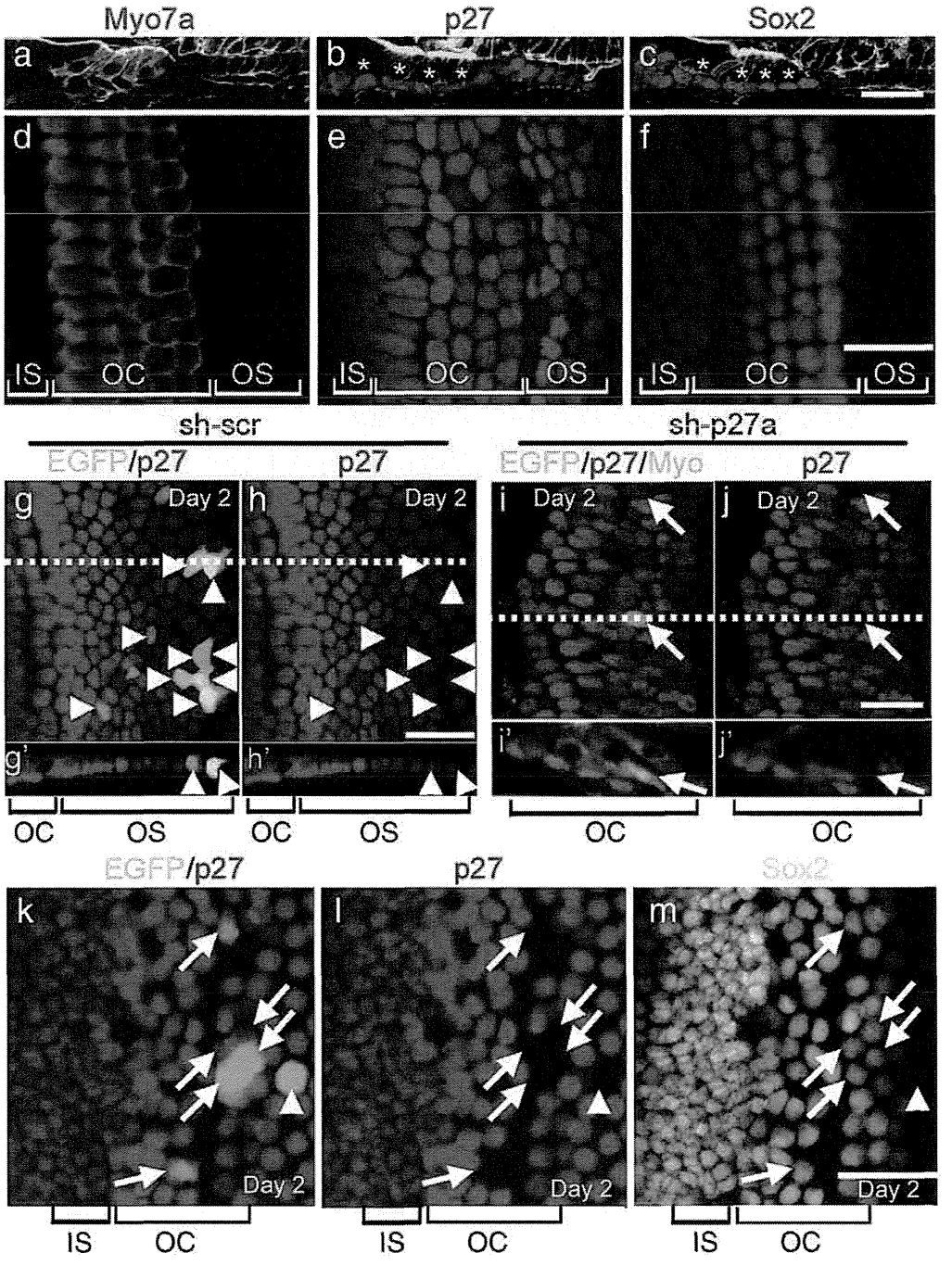


**Fig. 2.** Knockdown of $p27^{kip1}$ expression by RNAi occurred in supporting cells. Expression of myosin VIIa, $p27^{kip1}$ and Sox2 in sections (a–c) or in whole-mounts (d–f) are shown. Green fluorescence in a-c shows phalloidin staining. Asterisks in b, c indicate the location of hair cells. In cochlear epithelia transfected with sh-scr (g, h), EGFP+ cells (arrowheads) express $p27^{kip1}$. Cross-section images along with white dotted lines in g–j show in g'–j'. In cochlear epithelia transfected with sh-p27a (i–m), EGFP+ cells (arrows) are negative for $p27^{kip1}$. Double-labeling for myosin VIIa and $p27^{kip1}$ demonstrates the location of a transfected cell (arrow in I') corresponding to the supporting cell. Double-labeling for Sox2 and $p27^{kip1}$ (k–m) demonstrates the expression of Sox2 in EGFP+, $p27^{kip1}$- cells (arrows), indicating that $p27^{kip1}$ silencing occurs in supporting cells. A part of EGFP+, $p27^{kip1}$- cells lacks Sox2 expression (arrowhead in k–m). Myo7a, Myosin VIIa; IS, inner sulcus; OC, organ of Corti; OS, outer sulcus. Scale bars = 30 μm.

explanations for this. One is that insufficient suppression of $p27^{kip1}$, which was not enough for S-phase reentry, occurred in 70% of transfected cells. Another is that other cell-cycle inhibitors compensate the function of $p27^{kip1}$.

*Mitosis in SCs induced by RNAi with $p27^{kip1}$*

We performed time-lapse observations and propidium iodide (PI) staining in order to document the characteristic morphology for mitosis in SCs in which the $p27^{kip1}$ had been silenced. Two days after the introduction of a mixture of sh-p27a and pEGFPN-1, time-lapse observations of EGFP+ cells demonstrated mitosis in SCs within the explants (Fig. 5a, b, S1). We observed 10 EGFP+ cells in the outer sulcus region. In five out of the 10 EGFP+ cells that were recorded, the cells became rounded in shape and then divided into two daughter cells, which stained for BrdU but did not show any labeling for $p27^{kip1}$ (Fig. 5c, d). In addition, cross sections clearly showed nuclear migration to the luminal portion of the SCs (Fig. 5c', d'). During this process, PI staining of the nuclear chromatin demonstrated that there was segregation of the chromosomes in

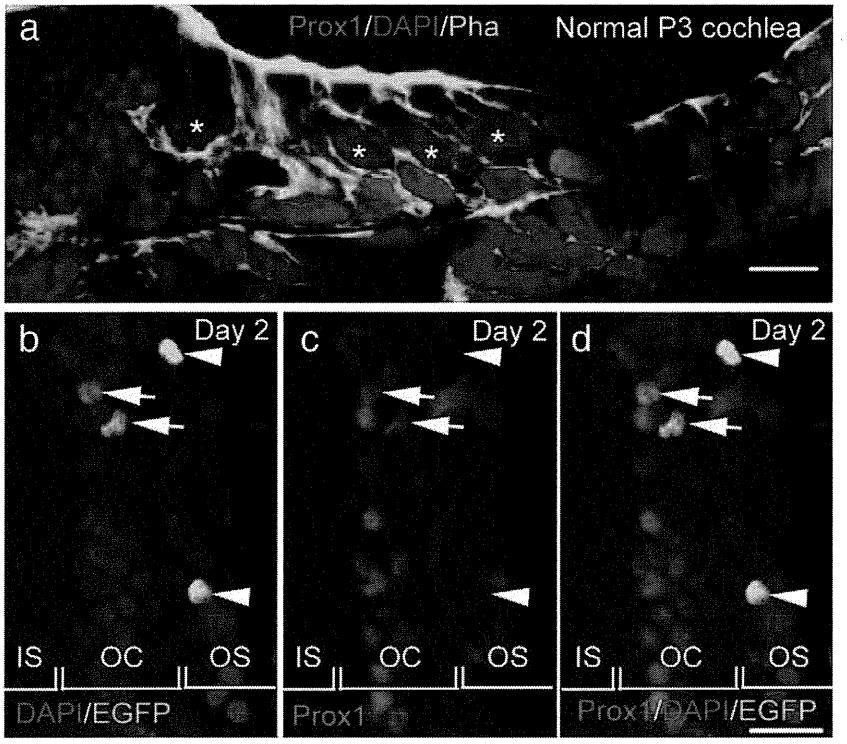


**Fig. 3.** Transfection in Prox1-positive supporting cells. In normal P3 cochlear epithelia, Prox1 expression (red) is seen in pillar cells and Deiters' cells (a). Green fluorescence in a shows phalloidin staining (Pha), and blue shows nuclear staining with DAPI. Asterisks in a indicate the location of hair cells. Some EGFP+ cells exhibit Prox1 expression (arrows in b–d), while other EGFP+ cells in the outer sulcus are negative for Prox1 (arrowheads in b–d). IS, inner sulcus; OC, organ of Corti; OS, outer sulcus. Scale bars = 20 μm.

the EGFP+ cells (Fig. 5e, f). Thus, these results showed that silencing of the $p27^{kip1}$ expression in post-mitotic SCs induced mitosis of the SCs in postnatal cochlear epithelia. This provides direct evidence that $p27^{kip1}$ plays a central role in controlling the proliferation of the SCs in neonatal cochleae. White et al. (2006) have reported that the capacity of SCs for proliferation is diminished depending on ages. Therefore, further experiments are required to date the efficacy of RNAi for $p27^{kip1}$ for induction of SC proliferation in adult mouse cochleae.

*Fate of SCs after $p27^{kip1}$ silencing*

To examine the effect of silencing $p27^{kip1}$ expression on the survival of post-mitotic SCs, we counted the number of EGFP+ cells in the cochlear epithelia that had been introduced in a mixture of pEGFPN-1 and sh-p27a or sh-scr (Fig. 6). Quantitative analysis of the EGFP+ cell survival demonstrated no significant differences in the number of surviving cells among culture periods in explants transfected with sh-scr, while there were significant reduction in the number of transfected cells was found in explants transfected with sh-p27a (Fig. 6). The number of EGFP+ cells on day 5 or 7 was significantly lower than that on day 1 or 2. These findings indicate that introduction of sh-p27a induced the loss of transfected SCs. We also examined the numbers of EGFP+, BrdU+ cells, cell-cycle reentering cells, in explants transfected with a mixture of sh-p27a and pEGFPN-1. BrdU incorporation was not found in EGFP+ cells on day 1, while on days 2-7, EGFP+, BrdU+ cells were observed in explants that had been introduced sh-p27a. There were significant differences in the number of EGFP+, BrdU+ cells between day 2 and day 3, 5, or 7 (Fig. 6). Fig. 6 indicates that the reduction of EGFP+ cells between day 2 and 3 mainly caused by the reduction of EGFP+, BrdU+ cells, and that the reduction of EGFP+ cells between day 3 and 5 was due to the loss of EGFP+, BrdU- cells. Therefore, both reentry of cell cycle by silencing $p27^{kip1}$ expression and silencing $p27^{kip1}$ expression itself may induce degeneration of transfected SCs.

We then investigated the cell death mode that occurred after silencing $p27^{kip1}$ expression. Immunohistochemical labeling for cleaved caspase 3 along with PI staining was performed in the explants 3 days after introduction of a mixture of sh-p27a and pEGFPN-1. The activation of caspase 3 was identified in 9/327 EGFP+ cells in six explants (Fig. 7a). PI staining showed the fragmentation of nuclear chromatin in EGFP+ and cleaved caspase 3+ cells (Fig. 7b). In addition, we examined the effects of the addition of a caspase 3 inhibitor to the culture medium. Addition of the caspase 3 inhibitor significantly increased the number of EGFP+ cells in explants transfected with sh-p27a (two-way factorial ANOVA, $p<0.0001$, Fig. 8). However, the caspase 3 inhibitor did not completely prevent the loss of EGFP+ cells, as over time, the explants treated with the caspase 3 inhibitor exhibited a decrease in their numbers (Fig. 8). All these results indicated that silencing the $p27^{kip1}$ expression in post-mitotic SCs initiated apoptosis in at least some, but not all of the cells. These results are consistent with previous data reported for apoptosis in mouse hair cells after the deletion of pRb (Mantela et al., 2005; Sage et al., 2005; Weber et al., 2008), $p19^{ink4d}$ (Chen et al., 2003) or both $p19^{ink4d}$ and $p21^{cip1}$ (Laine et al., 2007). On the other hand, the results indicate that other mechanisms rather than degradation via apoptosis are involved in the loss of transfected SCs. Hence, further investigations are necessary to reveal mechanisms for the loss of transfected SCs.

On the other hand, even at 7 days after the introduction of a mixture of sh-p27a and pEGFPN-1, EGFP+, BrdU+ cells were still observed in cochlear epithelia that had been transfected with sh-p27a. To examine the potential of silencing $p27^{kip1}$ expression for trans-differentiation of SCs into hair cells, specimens that had been transfected with sh-p27a were immunohistochemically labeled for myosin VIIa. The results showed that there was no myosin VIIa

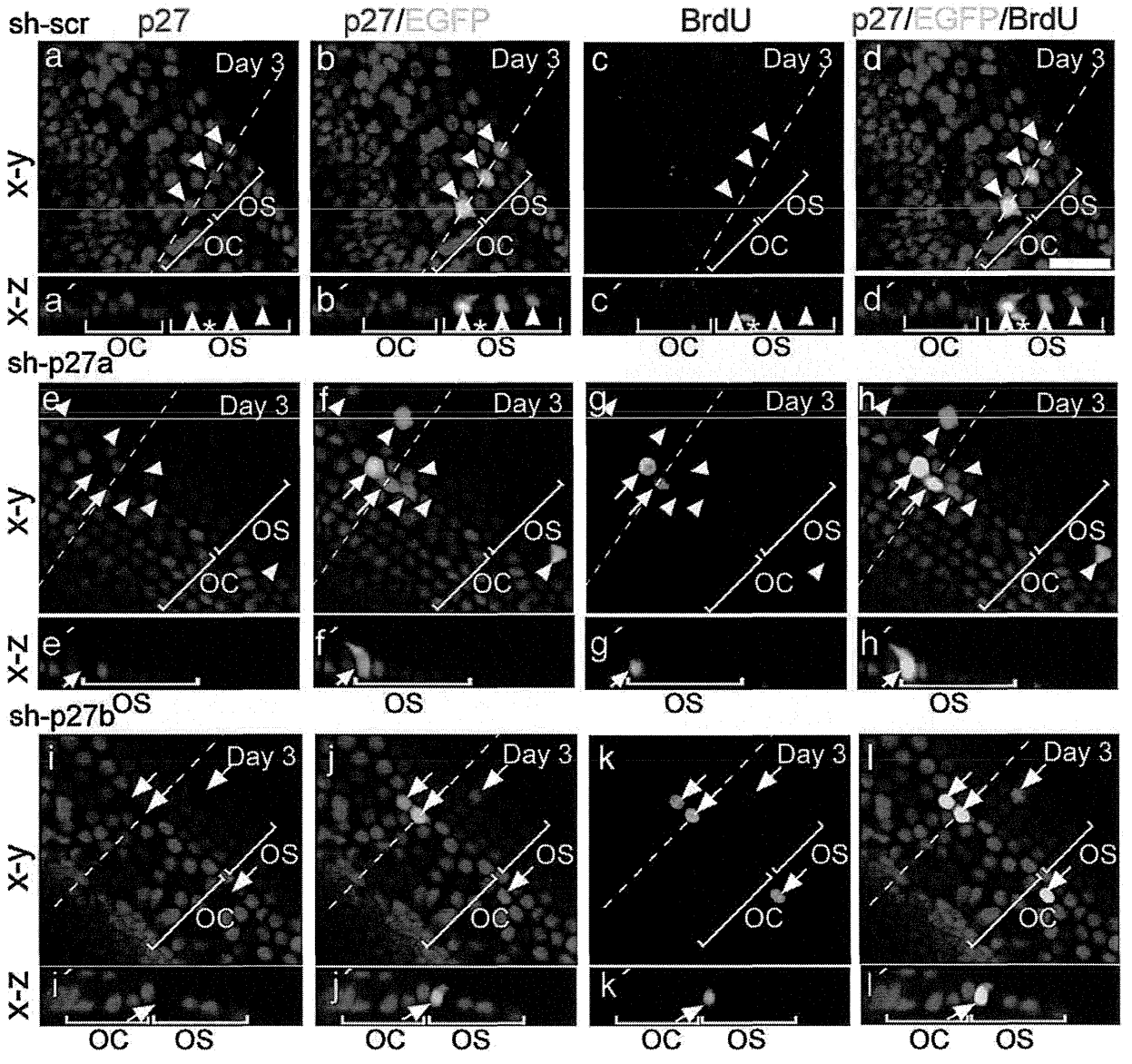


**Fig. 4.** Supporting cells silenced $p27^{kip1}$ by RNAi reenter S-phase. In cochlear epithelia following introduction of sh-scr, EGFP+ cells exhibit expression of $p27^{kip1}$ and are negative for BrdU (arrowheads in a–d). In cross-section images (a'–d') along with white dotted lines in a–d, a cell located underneath the cochlear epithelium shows BrdU incorporation (asterisk). In cochlear epithelia following introduction of sh-p27a (e–h) or sh-p27b (i–l), some of EGFP+, $p27^{kip1}$- cells exhibit BrdU incorporation (arrows). Other EGFP-positive cells (arrowheads in e–h) show silencing of $p27^{kip1}$, but no incorporation of BrdU. OC, organ of Corti; OS, outer sulcus. Scale bar = 30 μm.

labeling noted in the EGFP+ cells on days 5 and 7 (data not shown). These findings indicate that no SCs in which the $p27^{kip1}$ expression had been silenced underwent the trans-differentiation into hair cells. On the other hand, a separate study that used dissociated SCs showed the ability of post-mitotic SCs to trans-differentiate into hair cells in combination with the downregulation of $p27^{kip1}$ *in vitro* (White et al., 2006). Therefore, it appears that further manipulations are required in order to achieve hair cell regeneration in tissue.

When there is manipulation of Notch signaling by gene transfer (Kawamoto et al., 2003) or by pharmacological inhibitors (Yamamoto et al., 2006), the formation of ectopic hair cells in the outer sulcus region was observed, suggesting that SCs in this region are able to retain their ability to trans-differentiate into hair cells. In the avian auditory epithelium, the loss of hair cells is a key trigger that leads to the conversion of SCs to hair cells, a process for which Notch signaling is also involved (Stone and Rubel, 1999; Cafaro et al., 2007). In the mammalian cochlear epithelium, transient activation of Notch signaling has been observed in SCs following hair cell loss (Hori et al., 2007; Batts et al., 2009), suggesting that additional manipulation of Notch signaling in SCs could possibly contribute to the regeneration of hair cells once there is induction of SC proliferation by RNAi with $p27^{kip1}$.

Sage et al. (2005) demonstrated that there was proliferation of SCs in the cochlear epithelia of pRb−/− mice, indicating that pRb can be a target to induce cell-cycle reentry of post-mitotic SCs in tissue. However, pRb expression is undetectable in SCs in post-natal cochlear epithelia in normal mice (Mantela et al., 2005). Therefore, pRb expression does not appear to be an attractive candidate for induction of mitosis in post-natal SCs. In contrast, post-natally in normal mice, the $p27^{kip1}$ expression is strong and stable in the SCs (Chen and Segil, 1999; Löwenheim et al., 1999; Endo et al., 2002; White et al., 2006). Based on these reports, we considered $p27^{kip1}$ to be an appropriate target for induction of SC proliferation in the mammalian cochlear epithelium.

In conclusion, this is the first report showing induction of mitosis in post-mitotic mammalian SCs in tissue by RNAi targeting of $p27^{kip1}$. The present findings indicate that $p27^{kip1}$ expression is sufficient for

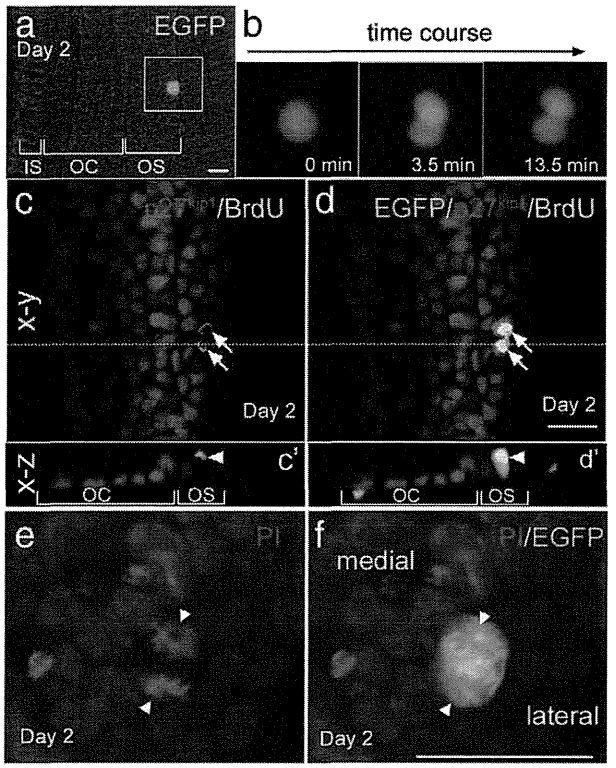


**Fig. 5.** Mitosis in supporting cells silenced $p27^{kip1}$ by RNAi. Time-lapse observation demonstrates division of sh-p27a-transfected supporting cells (a, b). A dividing cell expressing EGFP is positive for BrdU, but not for $p27^{kip1}$ (arrows in c, d). Cross-section images along with white dotted lines in c, d show migration of a BrdU+ nucleus to the luminal surface of the supporting cell (arrowheads in c', d'). An EGFP+ supporting cell in the outer sulcus region exhibits the segregation of chromosomes (arrowheads in e, f). PI, Propidium iodide, IS, inner sulcus; OC, organ of Corti; OS, outer sulcus. Scale bars = 30 μm.

maintaining the post-mitotic state of the SCs in tissue, and that RNAi is an efficient strategy for knockdown of the expression of $p27^{kip1}$ in the SCs of post-natal mammalian cochlear epithelia. On the other hand, our data have also identified obstacles that need to be overcome in order to achieve hair cell regeneration via the stimulation of SC proliferation. The most critical of these factors is the activation of the apoptotic pathways in SCs after silencing the expression of $p27^{kip1}$. Induction of trans-differentiation of the SCs into hair cells is also indicated obstacles to be overcome. Therefore, further manipulations

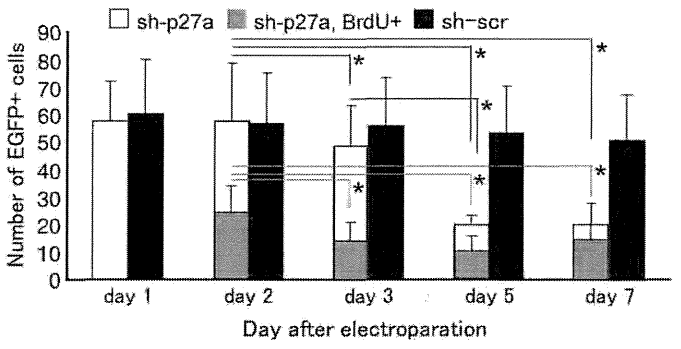


**Fig. 6.** Effects of silencing $p27^{kip1}$and cell-cycle reentry on transfected supporting cell survival. The surviving EGFP+ cell numbers in sh-scr-transfected explants (black column) show no significant alteration among culture periods, while those in sh-p27a-transfected explants (white column) significantly decreased over time. Significant decreases in numbers EGFP+, BrdU+ cells that have reentered cell-cycle, in sh-p27a-transfected explants (grey column)are observed on days 3–7 in comparison with day 2. Asterisks indicate statistical significance with the Tukey–Kramer test. Bars represent standard deviation.

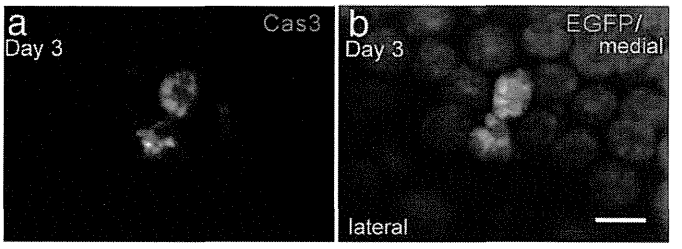


**Fig. 7.** Activation of caspase 3 in supporting cells that had been silenced $p27^{kip1}$ in the outer sulcus region. The expression of cleaved caspase 3 is found in sh-p27a-transfected supporting cells (a). PI staining exhibits the fragmentation of nuclear chromatins in sh-p27a-transfected supporting cells expressing EGFP (b). Scale bar = 10 μm.

are required for preventing apoptosis and induction of trans-differentiation into hair cells to achieve hair cell regeneration by downregulating $p27^{kip1}$.

## Experimental methods

### *Animals*

ICR mice (Japan SLC Inc., Hamamatsu, Japan) were maintained at the Institute of Laboratory Animals, Graduate School of Medicine, Kyoto University, Japan. Experimental protocols were approved by the Animal Research Committee of Kyoto University Graduate School of Medicine (MedKyo07062), and complied with the US National Institutes of Health (NIH) Guidelines for the Care and Use of Laboratory Animals.

### *Explant culture*

P3 ICR mice were deeply anesthetized with carbon dioxide and decapitated. The temporal bones were dissected out and the cochleae removed from the surrounding tissue in 0.01 M phosphate-buffered saline (PBS), pH 7.4, which was supplemented with 0.2% glucose. The lateral walls were removed from the cochleae and the cochlear epithelia were dissected from the cochlear modiolus and placed intact on sterile membranes in culture inserts (12 mm Millicell CM, Millipore, Billerica, MA). These explants were maintained in 24-well culture plates (Iwaki, Tokyo, Japan) in minimum essential medium (MEM; Invitrogen, Carlsbad, CA) supplemented with 3 mg/ml glucose and 0.3 mg/ml penicillin G potassium salt (Nacalai Tesque, Kyoto, Japan), at 37 °C in a humidified atmosphere of 95% air and 5% $CO_2$ for 24 h. The cultured explants were then used for the electroporation experiments.

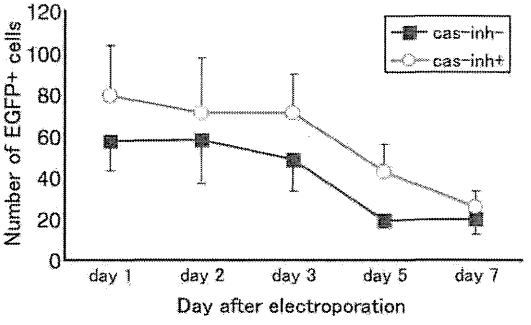


**Fig. 8.** Effect of a caspase 3 inhibitor on the number of surviving supporting cells following $p27^{kip1}$silencing. Closed squares show the numbers of EGFP+ cells in sh-p27a-transfected explants cultured without a caspase 3 inhibitor, and open circles show those with a caspase 3 inhibitor. An overall effect of application of a caspase 3 inhibitor is significant at $p<0.001$ with two-way factorial ANOVA, no significant differences in the numbers of EGFP+ cells were identified with pair-wise comparisons with Tukey–Kramer test. Bars represent standard deviation.

*Plasmids*

ShRNAs are RNA sequences that make tight hairpin turns and can silence gene expression via RNAi (Paddison et al., 2002). These sequences are expressed in vectors and can be used to target the $p27^{kip1}$ coding sequence (sh-p27) or to act as a control scrambled sequence (sh-scr). The two different sh-p27s prepared for this experiment were sh-p27a and sh-p27b. The sequences were 5′-AGACAATCAGGCTGGGTTA-3′ for sh-p27a, 5′-GAAGCGACCTGCTGCA-GAA-3′ for sh-p27b and 5′-TACGCGCATAAGATTAGGG-3′ for the sh-scr control sequence. These complementary sequences were inserted into the mU6 pro vector. The efficacy of sh-p27s in silencing the $p27^{kip1}$ expression in neuronal cells has been previously demonstrated (Kawauchi et al., 2006). pEGFP-N1 and pDsRed-Express-N1 vectors were purchased from Clontech (Palo Alto, CA). Each plasmid DNA was propagated in DH5α *Escherichia coli* and purified using an Endo Free Plasmid Maxi Kit (Qiagen, Valencia, CA). The yield and purity of the plasmid DNA was evaluated using an Ultrospec 3300pro spectrophotometer (GE Healthcare, Tokyo, Japan).

*Electroporation*

For the electroporation experiments, we prepared four kinds of plasmid mixtures that included, pDsRed-Express-N1 and pEGFP-N1, sh-p27a and pEGFP-N1, sh-p27b and pEGFP-N1 and sh-scr and pEGFP-N1. All vectors were diluted in electroporation buffer (125 mM NaCl, 5 mM KCl, 1.5 mM $MgCl_2$, 10 mM glucose, 20 mM HEPES, pH 7.4) to a concentration of 1.5 mg/ml. A CUY21 electroporator (Nepa Gene, Chiba, Japan) was used to transfer the plasmid mixtures into the auditory epithelial cells from the explant cultures. Culture inserts were placed on the lower platinum electrode, with 10 μl of the plasmid DNA solution then applied between them. Eight rectangular pulses (14 V, 50 ms duration at 100-ms intervals) were passed from the upper to the lower electrodes, followed by an additional eight pulses that were applied from the lower to the upper electrodes. Afterwards, explant cultures were maintained in culture medium supplemented with 3 μg/ml BrdU (Sigma-Aldrich, St. Louis, MO) for 1–7 days. The culture medium was changed daily. Ten cochlear epithelia were used for a single culture, with ten independent cultures performed.

*Immunohistochemistry*

Explants were fixed in 4% paraformaldehyde (PFA) in PBS for 15 min at room temperature, washed with 0.2% Triton-X 100 in PBS (Triton-PBS) and stained as whole mounts. After blocking with 10% normal goat serum in Triton-PBS at 4 °C for 60 min, the explants were incubated overnight with the following primary antibodies: anti-mouse $p27^{kip1}$ rabbit polyclonal antibody (1:500; Lab Vision, Fremont, CA), anti-myosin VIIa rabbit polyclonal antibody (1:500; Proteus Bioscience, Ramona, CA), anti-Sox2 goat polyclonal antibody (1:500, Santa Cruz Biotechnology, Inc., Santa Cruz, CA), anti-Prox1 rabbit polyclonal antibody (1:1000; Chemicon, Temecula CA), anti-BrdU mouse monoclonal antibody (1:100; Becton Dickinson, Franklin Lakes, NJ), and anti-cleaved caspase-3 mouse monoclonal antibody (1:100; #9661S, Cell Signaling Technology, Danvers, MA). Alexa Fluor 594-conjugated anti-rabbit antibody, Alexa Fluor 633-conjugated anti-mouse, or anti-rabbit antibody (1:500; Invitrogen) was used as the secondary antibody and Vectashield (Vector Laboratories, Burlingame, CA) was used for mounting the samples. For BrdU staining, the specimens were pre-treated in 2N HCl for 20 min at 37 °C, and neutralized with 0.01M PBS (pH 8.5) for 10 min at room temperature. To label for both myosin VIIa and $p27^{Kip1}$ simultaneously, a Zenon™ Alexa Fluor 647 Rabbit IgG Labeling Kit (Invitrogen) was used. PI (Invitrogen) was used to stain nuclear chromatin. Images were acquired using a confocal laser scanning system (TCS SP2, Leica Microsystems, Wetzlar, Germany).

*Co-transfection efficiency*

To examine the efficiency of co-transfecting two different plasmids, we used five explants that were transfected with a mixture of pEGFPN-1 and pDsRed-Express-N1 vectors. To identify the location of the SCs in the cochlear epithelia, the explants were labeled immunohistochemically for $p27^{kip1}$ 1 day after the electroporation. We then quantified the number of $p27^{kip1}$+ cells that were also EGFP+ and/or DsRed+.

*Silencing $p27^{kip1}$ expression in SCs by RNAi*

To examine the efficiency of silencing $p27^{kip1}$ in sh-p27-transfected SCs, explants were transfected with a mixture of sh-scr and pEGFPN-1, sh-p27a and pEGFPN-1 or sh-p27b and pEGFPN-1 2 days prior to being immunolabeled for $p27^{kip1}$ ($n=5$ in each condition). We then quantified the number of $p27^{kip1}$-EGFP+ and EGFP+ cells in the cochlear epithelia. To examine the location of EGFP+ cells in the cochlear epithelium, we counted the number of EGFP+ cells in the outer sulcus region, in the organ of Corti and in the inner sulcus region in sh-p27a-transfected specimens.

To confirm that EGFP+ and $p27^{kip1}$-cells were SCs after the knockdown of $p27^{kip1}$, immunohistochemistry for $p27^{kip1}$ and myosin VIIa or Sox2 was performed in explants 2 days after sh-p27a introduction ($n=5$ for myosin VIIa, $n=4$ for Sox2). To examine the efficacy of transfection in pillar cells and Deiters' cells, immunostaining for Prox1 was performed in explants 2 days after sh-p27a introduction ($n=7$). In order to demonstrate normal distributions of these molecules, we used frozen sections or whole mounts of P3 ICR mouse cochleae after 1 day *in vitro* ($n=10$) for the immunohistochemistry controls. At the end of the staining procedures, we used FITC-phalloidin (Invitrogen) to counterstain the specimens.

*S-phase reentry of SCs by silencing $p27^{kip1}$*

To examine the effect of silencing $p27^{kip1}$ expression on the S-phase reentry of SCs, we used cochlear explants that were introduced a mixture of sh-p27a ($n=9$), sh-p27b ($n=5$) or sh-scr ($n=5$) and pEGFPN-1 3 days prior to labeling the explants for $p27^{kip1}$ and BrdU. We then counted the number of BrdU+ EGFP+ cells and EGFP+ cells for each group.

*Mitosis in SCs induced by RNAi with $p27^{kip1}$*

To examine the effect of $p27^{kip1}$ silencing on SC division, we used cochlear explants that were introduced a mixture of sh-p27a and pEGFPN-1 ($n=10$) 2 days prior to making time-lapse recordings of the explants using the BZ-9000 system (Keyence, Osaka, Japan). In the different explants, still images were captured for 10 EGFP-expressing cells. Immediately after the time-lapse observations were recorded, the specimens were fixed with 4% PFA for 15 min at room temperature, and then stained immunohistochemically for $p27^{kip1}$ and BrdU or with PI.

*Fate of SCs after $p27^{kip1}$ silencing*

To determine the effect of $p27^{kip1}$ silencing on the survival and differentiation of post-mitotic SCs, mixtures of sh-p27 and pEGFPN-1 or sh-scr and pEGFPN-1 were introduced into cochlear explants at 1, 2, 3, 5 and 7 days ($n=5$–10) prior to the counting of the number of EGFP+ or EGFP+, BrdU+ cells.

Six explants into which a mixture of sh-p27a and pEGFPN-1 had been introduced 3 days earlier were labeled immunohistochemically for cleaved caspase 3 and stained with PI in order to investigate the

activation of the apoptotic pathways. In addition, we also clarified the caspase 3-dependency of SC death following the silencing of $p27^{kip1}$ expression by examining explants that were cultured in medium supplemented with 100 μM Caspase-3 inhibitor III (Calbiochem, San Diego, CA) after a mixture of sh-p27a and pEGFPN-1 had been introduced. The numbers of EGFP+ cells after 2–7 days of culturing were counted ($n=5$ for each time point).

To examine the trans-differentiation of SCs into hair cells after silencing the $p27^{kip1}$ expression, myosin VIIa was labeled immunohistochemically in explants into which a mixture of sh-p27a and pEGFPN-1 had been introduced 5 or 7 days earlier ($n=5$ for each condition). Results were used to examine the trans-differentiation of SCs into hair cells after silencing the $p27^{kip1}$ expression.

*Statistical analysis*

The effects of silencing $p27^{kip1}$ expression and inhibiting caspase 3 on the survival of EGFP+ cells in auditory epithelia were examined using a two-way factorial analysis of variance (ANOVA). When an interaction was determined to be significant, pair-wise comparisons were analyzed using the Tukey–Kramer test for multiple comparisons. A one-way factorial ANOVA with the Tukey–Kramer test was used for analysis of differences for the number of EGFP+, BrdU+ cells among cultured periods in cochlear explants that were introduced a mixture of pEGFPN-1 and sh-p27a. The data was presented as the means ± standard deviations.

## Acknowledgments

This study was supported by a Grant-in-Aid for Scientific Research from the Ministry of Education, Culture, Sports, Science and Technology of Japan and by a Grant-in-Aid for Researches on Sensory and Communicative Disorders from the Ministry of Health, Labour and Welfare of Japan. We thank Tatsunori Sakamoto and Norio Yamamoto for critical review of this manuscript.

## Appendix A. Supplementary data

Supplementary data associated with this article can be found, in the online version, at doi:10.1016/j.mcn.2009.08.011.

## References

Batts, S.A., Shoemaker, C.R., Raphael, Y., 2009. Notch signaling and Hes labeling in the normal and drug-damaged organ of Corti. Hear. Res. 249, 15–22.
Cafaro, J., Lee, G.S., Stone, J.S., 2007. Atoh1 expression defines activated progenitors and differentiating hair cells during avian hair cell regeneration. Dev. Dyn. 236, 156–170.
Chen, P., Segil, N., 1999. p27 (Kip1) links cell proliferation to morphogenesis in the developing organ of Corti. Development 126, 1581–1590.
Chen, P., Zindy, F., Abdala, C., Liu, F., Li, X., Roussel, M.F., Segil, N., 2003. Progressive hearing loss in mice lacking the cyclin-dependent kinase inhibitor Ink4d. Nat. Cell Biol. 5, 422–426.
Corwin, J.T., Cotanche, D.A., 1988. Regeneration of sensory hair cells after acoustic trauma. Science 240, 1772–1774.
Elbashir, S.M., Harborth, J., Lendeckel, W., Yalcin, A., Weber, K., Tuschl, T., 2001. Duplexes of 21-nucleotide RNAs mediate RNA interference in cultured mammalian cells. Nature 411, 494–498.
Endo, T., Nakagawa, T., Lee, J.E., Dong, Y., Kim, T.S., Iguchi, F., Taniguchi, Z., Naito, Y., Ito, J., 2002. Alteration in expression of p27 in auditory epithelia and neurons of mice during degeneration. Neurosci. Lett. 334, 173–176.
Fire, A., Xu, S., Montgomery, M.K., Kostas, S.A., Driver, S.E., Mello, C.C., 1998. Potent and specific genetic interference by double-stranded RNA in *Caenorhabditis elegans*. Nature 391, 806–811.
Harper, J.W., 2001. Protein destruction: adapting roles for Cks proteins. Curr. Biol. 11, R431–435.
Hori, R., Nakagawa, T., Sakamoto, T., Matsuoka, Y., Takebayashi, S., Ito, J., 2007. Pharmacological inhibition of Notch signaling in the mature guinea pig cochlea. NeuroReport 18, 1911–1914.
Hume, C.R., Bratt, D.L., Oesterle, E.C., 2007. Expression of LHX3 and SOX2 during mouse inner ear development. Gene Expr. Patterns 7, 798–807.
Kawamoto, K., Ishimoto, S., Minoda, R., Brough, D.E., Raphael, Y., 2003. Math1 gene transfer generates new cochlear hair cells in mature guinea pigs in vivo. J. Neurosci. 23, 4395–4400.
Kawauchi, T., Chihama, K., Nabeshima, Y., Hoshino, M., 2006. Cdk5 phosphorylates and stabilizes p27kip1 contributing to actin organization and cortical neuronal migration. Nat. Cell Biol. 8, 17–26.
Kirjavainen, A., Sulg, M., Heyd, F., Alitalo, K., Ylä-Herttuala, S., Möröy, T., Petrova, T.V., Pirvola, U., 2008. Prox1 interacts with Atoh1 and Gfi1, and regulates cellular differentiation in the inner ear sensory epithelia. Dev. Biol. 322, 33–45.
Laine, H., Doetzlhofer, A., Mantela, J., Ylikoski, J., Laiho, M., Roussel, M.F., Segil, N., Pirvola, U., 2007. p19(Ink4d) and p21(Cip1) collaborate to maintain the postmitotic state of auditory hair cells, their codeletion leading to DNA damage and p53-mediated apoptosis. J. Neurosci. 27, 1434–1444.
Löwenheim, H., Furness, D.N., Kil, J., Zinn, C., Gültig, K., Fero, M.L., Frost, D., Gummer, A.W., Roberts, J.M., Rubel, E.W., Hackney, C.M., Zenner, H.P., 1999. Gene disruption of p27(Kip1) allows cell proliferation in the postnatal and adult organ of Corti. Proc. Natl. Acad. Sci. U. S. A. 96, 4084–4088.
Mantela, J., Jiang, Z., Ylikoski, J., Fritzsch, B., Zacksenhaus, E., Pirvola, U., 2005. The retinoblastoma gene pathway regulates the postmitotic state of hair cells of the mouse inner ear. Development 132, 2377–2388.
Oesterle, E.C., Campbell, S., Taylor, R.R., Forge, A., Hume, C.R., 2008. Sox2 and JAGGED1 expression in normal and drug-damaged adult mouse inner ear. J. Assoc. Res. Otolaryngol. 9, 65–89.
Paddison, P.J., Caudy, A.A., Bernstein, E., Hannon, G.J., Conklin, D.S., 2002. Short hairpin RNAs (shRNAs) induce sequence-specific silencing in mammalian cells. Genes Dev. 16, 948–958.
Roberson, D.W., Rubel, E.W., 1994. Cell division in the gerbil cochlea after acoustic trauma. Am. J. Otol. 15, 28–34.
Ruben, R.J., 1967. Development of the inner ear of the mouse: a radioautographic study of terminal mitoses. Acta Oto-laryngol., Suppl. 220, 221–244.
Ryals, B.M., Rubel, E.W., 1988. Hair cell regeneration after acoustic trauma in adult Coturnix quail. Science 240, 1774–1776.
Sage, C., Huang, M., Karimi, K., Gutierrez, G., Vollrath, M.A., Zhang, D.S., García-Añoveros, J., Hinds, P.W., Corwin, J.T., Corey, D.P., Chen, Z.Y., 2005. Proliferation of functional hair cells in vivo in the absence of the retinoblastoma protein. Science 307, 1114–1118.
Stone, J.S., Rubel, E.W., 1999. Delta1 expression during avian hair cell regeneration. Development 126, 961–973.
Sherr, C.J., Roberts, J.M., 1999. CDK inhibitors: positive and negative regulators of G1-phase progression. Genes Dev. 13, 1501–1512.
Weber, T., Corbett, M.K., Chow, L.M., Valentine, M.B., Baker, S.J., Zuo, J., 2008. Rapid cell-cycle reentry and cell death after acute inactivation of the retinoblastoma gene product in postnatal cochlear hair cells. Proc. Natl. Acad. Sci. U. S. A. 105, 781–785.
White, P.M., Doetzlhofer, A., Lee, Y.S., Groves, A.K., Segil, N., 2006. Mammalian cochlear supporting cells can divide and trans-differentiate into hair cells. Nature 441, 984–987.
Yamamoto, N., Tanigaki, K., Tsuji, M., Yabe, D., Ito, J., Honjo, T., 2006. Inhibition of Notch/RBP-J signaling induces hair cell formation in neonate mouse cochleas. J. Mol. Med. 84, 37–45.